C.P. No. 852

C.P. No. 852

MINISTRY OF AVIATION

AERONAUTICAL RESEARCH COUNCIL

CURRENT PAPERS

The Motion of Helicopter Blades at Low Rotor Speeds in High Winds

by

M. A. P. Willmer

LONDON: HER MAJESTY'S STATIONERY OFFICE

1966

TEN SHILLINGS NET

C.P. 852

September, 1963

THE MOTION OF HELICOPTER BLADES AT LOW ROTOR SPEEDS IN HIGH WINDS

by

M. A. P. Willmer

SUMMARY

A theory for predicting the behaviour of a rotor at low r.p.m. in a strong steady wind has been developed. Results have been obtained both for helicopters on the ground and on a rolling platform. It has been found that, under steady conditions and with the helicopter on the ground, serious blade deflections are not likely to occur. However, with a helicopter on a raised landing deck, it is possible for the 'cliff-edge' effect to be of major importance especially for helicopters with large rotors relative to the deck width. Finally the blade response to a vertical gust has been investigated and it has been shown that helicopter rotors are very susceptible to them.

Replaces A.R.C.25835. RAE TM Naval 181

CONTENTS

ILLUSTRATIONS

ILLUSTRATIONS (CONTD)

1 INTRODUCTION

For the effective operation of helicopters in the Royal Navy, it is necessary that they should be able to operate from ships over a wide range of sea and wind conditions. This includes the need for the rotors to be safely started and stopped in high winds. However, it is known that in such conditions, even ashore, large blade deflections can occur when the rotor speed is low. The cause of these deflections is not fully understood. The complete analytical solution to the problem is not possible at this stage, due to the complexity of the blade bending and flapping motions, when the blade is in contact with the droop stops during only part of the azimuth rotation. For this reason, this paper concentrates on certain aspects of the problem. In this way a better understanding of the causes of large blade deflections at low rotor speed can be obtained relatively quickly.

The first aspect to be examined is the problem of a helicopter in a steady wind on the ground. The rotor blades have been assumed to be fixed at the flapping hinge. At very low r.p.m., when the blade rests on the droop stops, this assumption will be valid. For typical helicopters this would cover a rotor speed range of 0 to about 50 r.p.m. Unfortunately, the aerodynamic forces on the blade in this range of rotor speeds are extremely difficult to calculate. Conventional rotor theory as given by Ref.1 say, becomes less accurate as the tip speed ratio increases beyond a value of about 0.6, as this theory does not take into account such phenomena as blade stalling or reversed flow. For the purposes of this paper it is necessary to consider tip speed ratios much greater than that where the theory of Ref.1 begins to fail. In order to progress further therefore, the assumption is made that at a sufficiently large tip speed ratio, the aerodynamic force on the retreating side of the rotor disc can be neglected. A comparison is given between this assumption and a more complicated theory being developed at Naval Air Department at the moment. In this way, the use of a very sophisticated rotor theory is avoided.

Secondly, the case of a helicopter aboard a frigate is investigated. The behaviour of the blades whilst stopping and starting during severe rolling motion has been examined. This is primarily the effect of rotor incidence changes and, since rolling angles are much greater than pitching motion, trouble with the blades is expected to be greatest when the relative wind blows from either port or starboard. The presence of the ship and the landing platform will then also affect the blade motion considerably, for there will be in these cases a type of 'cliff-edge' effect. This paper considers these factors and the calculations are mainly devoted to a study of the behaviour of the Whirlwind and Wasp helicopter rotors.

Thirdly, the effect of vertical gusts on the blade motion is examined. Again, in order to calculate reasonably swiftly the aerodynamic forces involved, it is necessary to make many severe assumptions. The gust is considered to hit the whole blade instantaneously and to remain during the subsequent motion. From the point of view of examining the susceptibility of a rotor to sharp changes in vertical velocity, it is expected that the assumptions used will be satisfactory.

2 A HELICOPTER IN A STEADY WIND ON THE GROUND

To begin the investigation of blade sailing, the case of a helicopter in a high steady wind was considered. Fig.1 shows a typical helicopter in a wind of speed V ft/sec blowing in the longitudinal direction of the aircraft. When the rotor is stationary, the blades will bend as shown and the purpose of this investigation is to see whether in slowing down or starting up there is sufficient excess bending for the blades to strike the tail boom. In practice the helicopter need not necessarily be facing into wind so that the deflections all the way round the rotor disc must be considered. It is to be expected that with only collective pitch applied, the blades will rise as they come into wind and fall as they retreat. Also as the rotor slows down, it is to be anticipated that the aerodynamic forces acting on the blades will only be significant on the advancing side where the incident velocity is greatest. At the rotor speed considered, below 50 r.p.m., the rotor will probably be resting on the droop stops for most of the cycle so that the equation of blade bending will have slightly different boundary conditions from that generally used in helicopter blade bending theory. For present purposes therefore, the bending equation of Ref. 2 is modified slightly. The datum line, with respect to which the blade deflection z is measured, is now taken to be a line through the blade root at the hub, see Fig.2. This figure which shows the situation at a typical azimuth angle ψ is thus basically the same as Fig.24 of Ref.3. Hence the equation of blade bending is

$$EI\frac{\partial^4 z}{\partial r^4} - \tfrac{1}{2} m \Omega^2 (R^2 - r^2)\frac{\partial^2 z}{\partial r^2} + mr\Omega^2\frac{\partial z}{\partial r} + m\frac{\partial^2 z}{\partial t^2} = \frac{dL}{dr} + mr\Omega^2\beta_o - mg \qquad (1)$$

it being assumed that EI is constant across the span.

The boundary conditions are

$$z = \frac{\partial z}{\partial r} = 0 \quad \text{at } r = 0$$

and

$$\frac{\partial^2 z}{\partial r^2} = \frac{\partial^3 z}{\partial r^3} = 0 \quad \text{at } r = R \qquad (2)$$

as the blade is assumed to behave like a cantilever beam at the origin. Before equation (1) can be solved the aerodynamic component $\frac{dL}{dr}$ has to be estimated. This is difficult to do accurately because of the magnitude of the tip speed ratios involved in the problem. A typical value of μ is given by a 30 kt wind, a blade radius of 20 ft and a rotor speed of 3 rads/sec, so that $\mu \simeq 0.85$.

On the advancing side of the disc the simple theory of Ref.1 gives the approximate equation

$$\frac{dL}{dr} = \tfrac{1}{2} a \rho c \left\{ (\Omega r + V \sin \psi)^2 \vartheta_o - (\mu - V \beta_o \cos \psi)(\Omega r + V \sin \psi) - \dot{z}(\Omega r + V \sin \psi) \right\} \quad (3)$$

for a rotor with no applied cyclic pitch control. On the retreating side, however, this equation is no longer valid because of reversed flow and blade stalling. Although a sophisticated aerodynamic theory can be developed to calculate the $\frac{dL}{dr}$ component, the time and labour involved is not warranted by the accuracy required at the present stage. Fortunately some reasonable approximations can be made which keep the estimation of $\frac{dL}{dr}$ fairly straightforward.

The $\dot{z}$ term of equation (3) represents the damping of the motion and as damping will always be present it was decided to assume that it is constant round the disc. The value of the constant was found from the vertical flight condition. Also, as the largest aerodynamic force will occur on the advancing side, it was decided to assume that the remaining terms of equation (3) were zero on the retreating side of the disc. Thus $\frac{dL}{dr}$ was taken to be given by

$$\frac{dL}{dr} = F(\psi) - \tfrac{1}{2} a \rho c \Omega r \dot{z} \quad (4)$$

where

$$F(\psi) = \tfrac{1}{2} a \rho c \left\{ (\Omega r + V \sin \psi)^2 \vartheta_o - (\mu - V \beta_o \cos \psi)(\Omega r + V \sin \psi) \right\} \quad 0<\psi<\pi$$

$$= 0 \quad \pi<\psi<2\pi \quad . \quad (5)$$

It should be noticed too that the induced velocity terms are neglected but, as μ is large, this assumption is again expected to be reasonable.

A comparison between the above theory and some unpublished work on an advanced rotor theory by Bramwell and Wilde at the R.A.E. is given in Fig.3. Also included are some results from the well known Squire theory[3]. The comparison is between the theoretical predictions of the blade flapping motion of stiff blades with the shaft held at a constant angle to the flow at high tip speed ratios. It can be seen that, above a μ of 0.5, the accuracy of the theory of Squire diminishes until, at a μ of 0.9, it is very poor. The new simple theory, on the other hand, gives reasonable agreement for the first harmonic flapping angle a_1, whilst all the coning angle predictions are of the same order

of accuracy. The new theory can be seen to give, therefore, a reasonable first order approximation for the large tip speed ratio cases.

Fourier analysis gives $F(\psi)$, the aerodynamic loading, in the form

$$F(\psi) = B_o(r) + \sum_{n=1}^{\infty} (B_n(r) \cos n\psi + A_n(r) \sin n\psi) \tag{6}$$

where details of the analysis are to be found in Appendix I. Only the first few terms in the series will be considered so that, from equations (1), (4) and (6), the equation of blade bending becomes

$$EI \frac{\partial^4 z}{\partial r^4} - \tfrac{1}{2} m \Omega^2 (R^2 - r^2) \frac{\partial^2 z}{\partial r^2} + mr \Omega^2 \frac{\partial z}{\partial r} + m \frac{\partial^2 z}{\partial t^2} + \tfrac{1}{2} a \rho c \Omega r \frac{\partial z}{\partial t}$$

$$= B_o(r) + \sum_{n=1}^{N} (B_n(r) \cos n\psi + A_n(r) \sin n\psi) + mr \Omega^2 \beta_c - mg \tag{7}$$

Following Ref.2, a non-dimensional spanwise coordinate x can be used, thus giving

$$\frac{\partial^4 z}{\partial x^4} - K(1 - x^2) \frac{\partial^2 z}{\partial x^2} + 2Kx \frac{\partial z}{\partial x} + \frac{2K}{\Omega^2} \frac{\partial^2 z}{\partial x^2} + \frac{Jx}{\Omega} \frac{\partial z}{\partial t}$$

$$= b_o(x) + \sum_{n=1}^{N} (b_n(x) \cos n\psi + a_n(x) \sin n\psi) + 2K Rx \beta_o - \frac{2Kg}{\Omega^2} \tag{8}$$

where

$$x = r/R$$

$$K = \frac{mR^4 \Omega^2}{2EI} \tag{9}$$

$$J = \frac{\tfrac{1}{2} a \rho c \Omega^2 R^5}{EI}$$

with boundary conditions

$$x = 0 \qquad z = \frac{\partial z}{\partial x} = 0$$

$$x = 1 \qquad \frac{\partial^2 z}{\partial x^2} = \frac{\partial^3 z}{\partial x^3} = 0 \; . \tag{10}$$

To solve equation (8), z was assumed to be of the form

$$z = z_o(x) + \sum_{n=1}^{N} (z_{nc}(x) \cos n\psi + z_{ns}(x) \sin n\psi) \tag{11}$$

and the solutions obtained using a digital computer.

As examples of typical helicopters, the Whirlwind and P531 (Wasp) were chosen. The behaviour of the Whirlwind rotor, which has a blade tip deflection of about $3\frac{1}{2}$ ft when stationary, was examined in a 30 kt wind for rotor speeds of 4 and 2 rads/sec. Fig.4 gives the results for z_o, z_{1C} and z_{1S}. Fig.5 shows the total blade deflections at the fore and aft positions. These results were calculated assuming that there was no twist on the blades and that the value of ϑ_o was that at the $\frac{3}{4}$ spanwise position. In the case of the 4 rads/sec rotor speed both the values for the new theory and the conventional theory are shown, see Fig.4. Here the value of μ is 0.49 and it can be seen that the agreement between the theories is quite good. Figs.6 and 7 show the corresponding results for the P531.

From Fig.5 it can be seen that the static deflection is not exceeded in either case so it would appear that in a steady wind there is no danger of the tailboom being struck by the rotor blade as it accelerates or slows down. It must be remembered that the above calculations assume zero cyclic variations of pitch and do not take into account any cyclic stick movements which the pilot could make to tilt the rotor disc.

3 A HELICOPTER ABOARD A ROLLING SHIP IN A STEADY WIND

3.1 Rigid blade flapping

The rotor speed will be high when a helicopter lands on a ship. Although the pilot will have taken advantage of a quiescent period in order to land, it is quite possible that in a rough sea the ship will roll violently shortly afterwards. In such cases the effect of a large roll will be either a large increase of flow up or down through the rotor depending on whether the roll is into or out of the relative wind. Because the rotor speed is high, rigid blade flapping can be considered. Fig.8 shows a helicopter with no applied cyclic control in a relative wind of V ft/sec blowing at right angles to the axis of roll. Defining the flapping angle β by

$$\beta = a_o' - a_1' \cos\psi - b_1' \sin\psi \qquad (12)$$

we have from Ref.4

$$a_o' = \tfrac{1}{2}\gamma\left[\frac{\vartheta_o}{4}(1+\mu^2) + \frac{\lambda}{3}\right] \qquad (13)$$

$$a_1' = \frac{\mu\left[\frac{8}{3}\vartheta_o + 2\lambda\right]}{1 - \frac{1}{2}\mu^2} \qquad (14)$$

and

$$b_1' = \frac{4\mu a_c}{3(1+\frac{1}{2}\mu^2)} \quad . \qquad (15)$$

From Ref.5 it has been shown that a better approximation for b_1' is given by

$$b_1' = \frac{1}{1+\frac{1}{2}\mu^2}\left[\frac{4}{3}\mu a_o + K\bar{v}_o\right] \quad . \qquad (16)$$

Fig.9 shows the results for the P531 helicopter where the blade flapping is calculated at azimuth stations 0, 90, 180 and 270 degrees for rolls of 5, 10 and 15 degrees. Again the value of ϑ_o was taken to be that at the $\frac{3}{4}$ spanwise position. It can be seen that, as μ increases, the range of possible flapping opens up considerably. Under normal operating conditions the rotor speed of the P531 is high, about 340 r.p.m., and thus a μ of 0.1 is not exceeded until a wind speed of 34 kts or more is encountered. Thus trouble is only likely to occur during the starting and stopping of the rotor when the higher tip speed ratios will be experienced.

If the incident wind blows at an angle α to the roll axis, the effect is given approximately by using a modified angle of roll φ', where φ' is given by

$$\varphi' = \varphi \sin\alpha \quad . \qquad (17)$$

The variation of φ' with α is given in Fig.10.

3.2 Blade motion at low rotor speed

It was shown in Fig.9 that, for some angles of roll and at sufficiently large tip speed ratios, severe flapping will be obtained. When the flapping motion becomes excessive, it will be resisted by stops at the hub. There will be periods

therefore, in the starting or stopping of a rotor, under adverse conditions of wind and roll, when the blades will hit against these stops and bend as cantilever beams. Such a motion is extremely difficult to analyse for it will be a combination of flapping and transient blade bending. When the rotor speed is decreased further, the cantilever beam motion will predominate and thus the blade motion will be given approximately by the equations of section 2. These equations can be readily used by suitable choice of the velocity through the rotor. Examples of the theory, however, will be left until after the 'cliff-edge' effect has been examined.

3.3 The 'cliff-edge' effect

When a helicopter lands on a ship, the rotor can no longer be assumed to lie in an undisturbed airflow moving with a given velocity. The streamlines near the ship, when the wind is from the side, are expected to be like those shown diagrammatically in Fig.11. They will rise on the upstream side and fall on the downstream side. A rotor in the airflow above the ship will experience this up and down flow and it is this phenomenon which is sometimes called the 'cliff-edge' effect.

To estimate how these changes of rotor flow affect the rotor behaviour, it is assumed that the ship can be replaced by a two dimensional cylinder of equivalent radius, see Fig.12. This equivalent radius is defined by

$$\bar{a}^2 = s^2 + d^2 \quad . \tag{18}$$

If h is the height of the rotor disc above the deck then the vertical and horizontal velocities at P are given by[6],

$$V_V = V \frac{\bar{a}^2}{r'^2} \sin 2\theta \tag{19}$$

$$V_H = V \left(1 - \frac{\bar{a}^2}{r'^2} \cos 2\theta\right) \tag{20}$$

where

$$r'^2 = (h + s)^2 + q^2 \tag{21}$$

and

$$\theta = \arctan\left[\frac{h + s}{q}\right] \quad . \tag{22}$$

Thus, when the blade is at azimuth angle ψ, the vertical velocity at the spanwise position r is obtained by putting

$$q = -r \cos \psi \quad . \tag{23}$$

Defining

$$k = \frac{h + s}{R} \tag{24}$$

$$x = r/R \tag{25}$$

$$b = \bar{a}/R \tag{26}$$

equation (19) becomes,

$$\frac{V_v}{V} = \frac{-2b^2 k x \cos \psi}{[k^2 + x^2 \cos^2 \psi]^2} \quad . \tag{27}$$

For simplicity, it is assumed that the cylinder's pressure does not affect the horizontal velocity so that

$$V_H = V \quad . \tag{28}$$

The accuracy of this approximation is expected to be at least as good as that of the assumption that the ship can be replaced by a theoretical two dimensional cylinder.

The expression for the vertical velocity given by equation (27) can be simplified further by assuming that the demoninator is always calculated with $\psi = 0$. Fig.13 shows the comparison for $x/R = \frac{1}{2}$. Thus following Ref.1, the effect on the first harmonic of rotor flapping can be shown to be an increase in the b_1' component of

$$\Delta b_1' = \frac{4\mu}{1 + \frac{1}{2}\mu^2} b^2 \, g(k) \tag{29}$$

where

$$g(k) = k \left\{ \log\left(1 + \frac{1}{k^2}\right) - \frac{1}{1 + k^2} \right\} \quad . \tag{30}$$

The function $g(k)$ is plotted in Fig.14 and the increase of b_1' in Fig.15 for two values of b^2. The value of k chosen is typical of a P531 onboard an Ashanti Class frigate.

In order to calculate the effect of the 'cliff-edge' contribution on the blade bending at high μ's, an additional term to the $\frac{dL}{dr}$ of equation (3) must be included. This additional term, which is due to the extra lift, is given by

$$\Delta \frac{dL}{dr} = -\tfrac{1}{2} \rho c a (\Omega r + V \sin \psi) \frac{2b^2 kV x \cos \psi}{[k^2 + x^2]} \quad . \tag{31}$$

By making the further assumption that x = 1 in the denominator, this extra term results in a slight modification to the function defined by equation (A.2). Also if the cyclic control movements are included so that the blade pitch is given by

$$\vartheta_o' = \vartheta_o - B_1 \sin \psi - A_1 \cos \psi \tag{32}$$

the function of (A.2) becomes

$$g_o = \vartheta_o x^2 - x [B_1 \mu + \lambda] + \tfrac{1}{2} \vartheta_o \mu^2 \tag{33}$$

$$g_s = 2\mu x \vartheta_o - \lambda \mu - B_1 x^2 - \tfrac{3}{4} \mu^2 B_1 \tag{34}$$

$$g_c = \mu x \beta_o + \tfrac{1}{4} \mu^2 A_1 - \tfrac{1}{2} \mu^2 A_1 - x^2 A_1 - \frac{2 b^2 k \mu x^2}{[1 + k^2]^2} \tag{35}$$

$$h_c = B_1 \mu x - \tfrac{1}{2} \mu^2 \vartheta_o \tag{36}$$

$$h_s = \tfrac{1}{2} \mu^2 \beta_o - A_1 \mu x - \frac{\mu^2 b^2 k x}{[1 + k^2]^2} \quad . \tag{37}$$

The effect of the assumption, that x = 1 in the denominator of equation (31), on the first harmonic of rigid blade flapping can be shown to change the g(k) of equation (30) to

$$g'(k) = \tfrac{1}{2} \frac{k}{(1 + k^2)^2} \quad . \tag{38}$$

This function is compared with g(k) in Fig.14; for values of k above 1.5 it is a very reasonable approximation.

Results for a P531 onboard a frigate of the Ashanti Class with 15° of roll in a 25 kt wind are given in Figs.16 and 17. The former gives the harmonics of the deflections and the latter the total deflections at ψ = 0, 90, 180 and 270 degrees. It can be seen that the maximum deflection is about 1 ft which can be reduced by the appropriate cyclic control movements. Thus, for operations from frigates, it can be seen that the P531 is reasonably satisfactory from the point of view of stopping and starting the rotor under difficult conditions.

On the other hand, the Whirlwind can be shown to be much less suitable because the larger blades bend very much more. Fig.18 shows the harmonics of blade bending for a Whirlwind aboard a frigate with no cyclic control in a 30 kt wind. The order of the magnitude of the deflections is now considerably increased. The effect of applying cyclic control is given in Fig.19 where A_1 is taken to be -5 degrees. In the case of the 4 rads/sec rotor speed both results from conventional aerodynamic theory and the new simple theory are shown. In Fig.20 the variation of the total tip deflection with azimuth is given. From these figures it can be seen that the static deflection is well exceeded as the rotor speed decreases even when large cyclic control movements are applied. Although in calculating the aerodynamic forces many severe assumptions have been made, it is thought that the results obtained are of sufficient accuracy to indicate the importance of the 'cliff-edge' effects.

The 'cliff-edge' effect will also influence the total lift on the rotor whilst the helicopter is hovering over the deck before landing. If the rotor head is at a point $(y', h + s)$ instead of $(0, h + s)$, see Fig.12, the vertical velocity at the point (x, ψ) corresponding to equation (27) is

$$\frac{V_v}{V} = \frac{2 b^2 k(y - x \cos \psi)}{[k^2 + (y - x \cos \psi)^2]^2} \qquad (39)$$

where

$$y = y'/R \ . \qquad (40)$$

The increase of lift per blade is given approximately by

$$\Delta F = \tfrac{1}{2} \rho a c \Omega^2 R^3 \int_0^1 (x + \mu \sin \psi) \left\{ \frac{2 b^2 k(\mu/y - x \cos \psi)}{[k^2 + (y - x)^2]^2} - \frac{\Delta v}{\Omega R} \right\} dx \qquad (41)$$

where Δv is the increase in the induced velocity. From equation (41) it can be shown that for Q blades the increase in rotor thrust with y is approximately

$$\Delta T = \frac{\frac{1}{2}\rho a c \mu \Omega^2 R^3 Q b^2 k y}{\left[1 + \frac{Q a \sigma}{\sqrt{\mu^2 + \bar{v}_c^2}}\right]} \left\{ \frac{1}{k^2} \left[\frac{1 - y}{(1-y)^2 + k^2} \right] + \frac{y}{k^3} \left[\tan^{-1} \left(\frac{1-y}{k} \right) - \tan^{-1}(y/k) \right] \right\} \qquad \ldots \quad (42)$$

This increase for a P531 helicopter landing on a frigate is plotted as a percentage of the all up weight in Fig.21. This increase was noticed during recent P531 trials aboard H.M.S. Undaunted. Theoretically there should be a corresponding downward rotor force at positions downwind of the centre of the deck, but the effect experienced was not nearly so pronounced. This can be explained by the fact that the streamlines tend to remain horizontal after passing over the deck due to the wake downwind of the ship. This phenomenon is shown diagrammatically in Fig.1 of Ref.7.

4 THE EFFECT OF A VERTICAL GUST ON THE ROTOR AT LOW R.P.M.

It was shown in section 2 that no serious blade deflections are expected to occur when a Whirlwind starts or stops its rotor in a steady high wind. As several accidents have been reported in the past due to abnormal rotor behaviour, it would seem as though the cause must lie in the field of the blade response to gusts. The analysis of such effects, particularly at low r.p.m., is extremely difficult and many assumptions have had to be made in order to progress.

Only vertical gusts have been considered for these are expected to produce the greatest effects and the assumption is made that at a given time the whole blade is affected by the gust which continues until after the peak response has been obtained. This time for a Whirlwind rotor will be less than a second in most cases. Also it is assumed that the rotating blade behaves like a stationary cantilever beam with increased stiffness so that the equation for the blade deflection is given by

$$EI' \frac{\partial^4 z}{\partial r^4} + m \frac{\partial^2 z}{\partial t^2} = \frac{dL}{dr} + m r \Omega^2 \beta_o - mg \qquad (43)$$

where EI' is the modified stiffness. For convenience in the estimation of the aerodynamic term $\frac{dL}{dr}$ on the retreating side of the disc, the azimuth angle is taken from the upwind position so that

$$\psi = \pi + \xi \ . \qquad (44)$$

On the part of the blade where the stall has not been reached, $\frac{dL}{dr}$ is given by

$$\frac{dL}{dr} = \tfrac{1}{2} \rho a c w^2 \alpha \qquad (45)$$

where α is the angle of incidence and w is the velocity of the air with respect to the blade neglecting the spanwise component. Thus

$$w^2 = (\Omega r - V \sin \xi)^2 + \left[\mu_G + V\left(-\beta_o + \frac{\partial z}{\partial r}\right)\cos \xi - \dot{z}\right]^2 \quad \ldots \quad (46)$$

and

$$\alpha = \vartheta_o + \frac{\mu_G + V \cos \xi \left(\frac{\partial z}{\partial r} - \beta_o\right) - \dot{z}}{\Omega r - V \sin \xi} \quad (47)$$

where the blade is immersed in an upward gust of μ_G ft/sec. For the stalled part of the blade, it is assumed that

$$\frac{dL}{dr} = \tfrac{1}{2} \rho a c w^2 \alpha_s \ . \quad (48)$$

The value of r where blade stalling commences is obtained from the equation

$$(\alpha_s - \vartheta_o)(\Omega r_s - V \sin \xi) = \mu_G + V\left(\frac{\partial z}{dr} - \beta_o\right)\cos \xi - \dot{z} \ . \quad (49)$$

It is to be noted that the sign of α_s depends upon whether the blade is stalled from above or below and, in cases of ambiguity, the most outboard stalling point was used.

In order to obtain a quick solution to equation (43), the response of the blade to the gust is considered in segments, each of $\bar{h}$ sec duration. These segments are chosen sufficiently small that in them sin ξ, cos ξ, $\dot{z}$ and $\frac{\partial z}{\partial r}$ can be regarded as constant in the aerodynamic force term. In order to provide continuity the terminal deflections and velocities of one segment become the starting values for the next. Also it has been assumed that in each segment, the blade deflection and velocity vary linearly with the radius so that, in the (i + 1)th segment,

$$\dot{z}_{i+1} = \dot{z}(R,i)\ r/R \qquad \left(\frac{\partial z}{\partial r}\right)_{i+1} = \frac{1}{R}\dot{z}(R,i) \quad (50)$$

and thus the velocity w and the incidence α are given by

$$w_{i+1}^2 = (\Omega r - V \sin \xi_{i+1})^2 + \left\{\mu_G + V\left(\frac{z(R,i)}{R} - \beta_o\right)\cos \xi_{i+1} - \frac{r}{R}\dot{z}(R,i)\right\}^2 \quad \ldots \quad (51)$$

$$\alpha_{i+1} = \vartheta_o + \frac{\mu_G + V \cos \xi_{i+1} \left(\frac{z(R,i)}{R} - \beta_o \right) - \frac{r}{R} \dot{z}(R,i)}{\Omega r - V \sin \xi_{i+1}} \qquad (52)$$

where ξ_{i+1} takes the mean value of the segment. Thus it can be seen that w_{i+1} and α_{i+1} are now purely fractions of r.

The damping of the motion is calculated as if the rotor was hovering. By neglecting blade deflection effects and taking the value at the $\frac{3}{4}$ spanwise position, equation (43) becomes

$$EI' \frac{\partial^4 z}{\partial r^4} + m \frac{\partial^2 z}{\partial t^2} + \bar{a}_1 \frac{\partial z}{\partial t} = \left(\frac{dL}{dr} \right)' + m r \Omega^2 \beta_o - mg \qquad (53)$$

where

$$\bar{a}_1 = \tfrac{3}{8} \rho a c \Omega R \ . \qquad (54)$$

The $\left(\frac{dL}{dr} \right)'$ term is now a function of r only for each small segment and it contains all the aerodynamic terms minus the damping. Thus it is possible to write the deflection in the form

$$z = z_o(r) + z_t(r,t) \qquad (55)$$

where

$$EI' \frac{\partial^4 z_t}{\partial r^4} + m \frac{\partial^2 z_t}{\partial t^2} + \bar{a}_i \frac{\partial z_t}{\partial r} = 0 \qquad (56)$$

and

$$EI' \frac{\partial^4 z_o}{\partial r^4} = \left(\frac{dL}{dr} \right)' + m r \Omega^2 \beta_o - mg \ . \qquad (57)$$

Using the non-dimensional radius x, the solution of equation (56) which represents the time variable component can be written in the form

$$z_t(x,t) = \sum_k A_k \left\{ \frac{\cosh \beta_k x - \cos \beta_k x}{\cosh \beta_k + \cos \beta_k} - \frac{\sinh \beta_k x - \sin \beta_k x}{\sinh \beta_k + \sin \beta_k} \right\} \cos(\omega_k t + \varphi_k) \, e^{-b_k t}$$

$$r = xR \qquad \ldots \ (58)$$

see Refs.8 and 9. The natural frequency of the kth mode, ω_k, is given by

$$\omega_k = \omega_{nk}\sqrt{1 - \lambda_k^2} \tag{59}$$

where the undamped natural frequency ω_{nk} and the damping factor are obtained from

$$\omega_{nk}^2 = \frac{\beta_k^4 \, EI'}{R^4 \, m} \tag{60}$$

$$2\lambda_k \, \omega_{nk} = \bar{a}_1/m = 2\bar{b} \quad . \tag{61}$$

From Ref.8 the values of the first three β_k are given as 0.600π, 1.49π and 2.50π. However, for present purposes, only the fundamental mode will be used so that $z_t(x,t)$ is given by

$$z_t(x,t) = A\bar{g}(x) \cos(\omega t + \varphi) \, e^{-\bar{b}t} \tag{62}$$

$$\bar{g}(x) = \left[\frac{\cosh \beta x - \cos \beta x}{\cosh \beta + \cos \beta} - \frac{\sinh \beta x - \sin \beta x}{\sinh \beta + \sin \beta}\right] \tag{63}$$

where β, ω and $\bar{b}$ have the appropriate values.

The modified stiffness, EI', is determined from the results quoted in Ref. 10 where a relationship between the natural frequency of the rotating blade in any one mode and the natural frequency of the stationary blade in that mode is given. Thus

$$\omega_k^2 = \omega_{ok}^2 + \varepsilon \, \Omega^2 \tag{64}$$

where ω_k = natural frequency of the rotating blade in the bth mode

ω_{ok} = natural frequency of the stationary blade in that mode

Ω = angular velocity of the blade

ε = factor depending on the blade and root condition.

As the stiffness of the blade, EI, and the natural frequency of the stationary blade are connected by

$$\omega_{ok}^2 = \frac{\beta_k^2 \, EI}{R^4 \, m} \tag{65}$$

it can be seen that the modified stiffness, EI', can be calculated from equations (59-61, 64 and 65) using $\varepsilon = 1.2$ from Ref. 10.

As the motion is considered in segments, each of $\bar{h}$ sec duration, the deflection of the blade tip in the ith segment can be obtained from equations (55) and (62) giving

$$z(R,i,t) = z_o(R,i) + A^{(i)} \, \bar{g}(1) \cos(\omega t + \varphi^{(i)}) \, e^{-\bar{b}t} \tag{66}$$

and hence

$$\dot{z}(R,i,t) = -A^{(i)} \, \bar{g}(1) \, [\bar{b} \cos(\omega t + \varphi^{(i)}) + \omega \sin(\omega t + \varphi^{(i)})] \, e^{-\bar{b}t} \, . \tag{67}$$

The constants $A^{(i)}$ and $\varphi^{(i)}$ are obtained from the initial conditions at the start of the ith segment. Thus

$$z(R,i+1,t) = z_o(R,i+1) + e^{-\bar{b}t}\Big\{[z(R,i) - z_o(R,i)] \cos \omega t + [z(R,i) - \bar{b}(z_o(R,i) - z(R,i)) \, \frac{\sin \omega t}{\omega}\Big\} \tag{68}$$

where t is calculated from the start of each segment and where z(R,i) are the calculated deflections at the end of the ith segment.

The azimuth position of the blade is given by either

$$\psi = \pi + \xi_o + \Omega[(i - 1) \, \bar{h} + t] \tag{69}$$

or

$$\xi_{i+1} = \xi_o + \bar{h}(i - \tfrac{1}{2}) \, \Omega \tag{70}$$

and where the blade is completely engulfed by the gust whilst at the azimuth position $(\pi + \xi_o)$. To complete the analysis it is necessary to determine that part of the deflection which is independent of t. From equation (57) we have for the ith segment

$$EI' \frac{\partial^4 z_o}{\partial r^4} = \tfrac{1}{2} \rho a c \left(\ell_2^{(i)} r^2 + \ell_1^{(i)} r + \ell_o^{(i)} \right) \left(r_o + \frac{q^{(i)}}{\Omega r - V \sin \xi_i} \right) + mr \Omega^2 \beta_o - mg \quad \ldots (71)$$

when the blade is not stalled and

$$EI' \frac{\partial^4 z_o}{\partial r^4} = \tfrac{1}{2} \rho a c \alpha_s \left(\ell_2^{(i)} r^2 + \ell_1^{(i)} r + \ell_o^{(i)} \right) + mr \Omega^2 \beta_o - mg \quad (72)$$

when it is. The value of $\ell_o^{(i)}$, $\ell_1^{(i)}$ and $\ell_2^{(i)}$ are given by

$$\ell_o^{(i)} = V^2 \sin^2 \xi_i + \left\{ \mu_G + V \cos \xi_i \left[-\beta_o + \frac{1}{R} z(R,i-1) \right] \right\}^2 \quad (73)$$

$$\ell_1^{(i)} = -2\Omega V \sin \xi_i - \frac{2\dot{z}(R,i-1)}{R} \left\{ \mu_G + V \cos \xi_i \left[-\beta_o + \frac{1}{R} z(R,i-1) \right] \right\} \quad (74)$$

$$\ell_2^{(i)} = \Omega^2 + \left[\frac{\dot{z}(R,i-1)}{R} \right]^2 \quad (75)$$

and

$$q^{(i)} = \mu_G + V \cos \xi_i \left[-\beta_o + \frac{1}{R} z(R,i-1) \right] . \quad (76)$$

The integration of equations (71) and (72) is straight forward and the constants of the integration are derived by the necessity for continuity in the deflections and the first three derivations at the point of stall together with the end conditions.

The calculations were made using $\bar{h} = 0.02$ sec, this interval was found to be sufficiently small for present purposes. Fig.22 shows the effect of a 5 ft/sec downward gust on a Whirlwind rotor in a 30 kt wind. The helicopter was

taken to be on the ground and several initial values of ξ were chosen. It can be seen that the rotor is extremely susceptible to the gust at the lower rotor speed.

Unfortunately it is extremely difficult to find information on the order of magnitude and the frequency of gusts at ground level. Such information will be closely connected with the landscape of the surrounding countryside as well as with obstacles which disturb the airstream.

A similar problem is encountered in the case of a helicopter aboard ship. Here the superstructure of the ship, when the relative airflow is in the appropriate direction, will cause a disturbed airflow. It is difficult, at this stage, to see how successful the assumption that the blade is completely and instantaneously swallowed by the gust will be in practice. The above work does show, however, that the rotor, particularly at low r.p.m., is very sensitive to sharp changes in the vertical velocity.

5 CONCLUSIONS

(1) A theory for predicting the behaviour of a rotor in a strong steady wind whilst starting or stopping has been developed. Results have been obtained both for helicopters on the ground and on rolling ships at sea.

(2) It has been found that, under steady conditions and with the helicopter on the ground, no serious blade deflections are likely to occur.

(3) For a helicopter with a large rotor, it has been found that the 'cliff-edge' effect can cause significant blade deflections. However, it has been shown that the operation of the P531 from ships should be quite satisfactory from this point of view.

(4) The effect of vertical gusts has also been investigated theoretically and, although several severe assumptions have had to be made, it has been shown that a rotor of the Whirlwind type is extremely susceptible to such gusts.

6 ACKNOWLEDGEMENT

The writer wishes to thank Dr. E. Wilde of N.A.D. for his assistance in the preparation of the computer programmes involved in this study.

REFERENCES

No.	Author	Title, etc
1	Stewart, W.	Higher harmonics of flapping on the helicopter rotor. A.R.C.15041, C.P.121

REFERENCES (CONTD)

No.	Author	Title, etc
2	Hufton, P.A. et al	General investigation into the characteristics of the C.30 Autogiro. A.R.C. R & M 1859. March 1939.
3	Squire, H. B.	The flight of a helicopter. A.R.C. R & M 1730.
4	Gessow, A. Myers, G.C.	Aerodynamics of the helicopter. The Macmillan Company, New York. 1952.
5	Stewart, W.	Helicopter control to trim in forward flight. A.R.C. R & M 2733. March 1950.
6	Glauert, H.	The elements of aerofoil and airscrew theory. The Cambridge University Press. 1926.
7	National Physical Laboratory	The industrial application of aerodynamic techniques. Notes on Applied Science No.2. 1952.
8	Karman, von T. Biot, M.	Mathematical methods in Engineering. McGraw Hill Book Co. Inc. New York and London. 1940.
9	Neumark, S.	Concept of complex stiffness applied to problem of oscillations with viscous and hysteretic damping. A.R.C. R & M 3269. Sept. 1957.
10	Jones, J.P.	The influence of the wake on the flutter and vibration of rotor blades. Aeronaut. Q. Vol.IX, Part 3, 1958 p.p.258-286.

SYMBOLS

a	lift curve slope
A_1, B_1	coefficients of feathering
c	blade chord
d	semi-width of platform
EI	flapwise stiffness
EI'	modified flapwise stiffness
g	acceleration due to gravity
h	height of rotor above platform
$\bar{h}$	interval of time
L	lift on the blade
m	mass
Q	number of blades
R	rotor radius
r	spanwise coordinates
r_s	position along the blade where stalling occurs
s	height of platform above sea level
ΔT	increase in total thrust due to 'cliff-edge' effect
t	time
u	velocity through rotor
μ_G	gust velocity
v	induced velocity
v_o	mean induced velocity/tip speed
V	wind velocity
x	non-dimensional spanwise coordinate
y'	sidewards displacement of helicopter from the centre of the platform

SYMBOLS (CONTD)

z	blade deflection
z_o	blade deflection which is independent of t
z_t	blade deflection which is a function of t
α_s	stalling angle
β_o	angle subtended by the blade at the root
β	flapping angle
γ	Lock's inertia No.
λ	coefficient of flow through the disc (pointing upwards)
μ	tip speed ratio
φ	angle of roll
ρ	air density
Ω	angular velocity of rotor
ψ	blade azimuth position measured from the downwind position in direction of motion
ϑ_o	collective pitch of blade
σ	solidity

APPENDIX 1

From equations (5), $F(\psi)$ becomes

$$F(\psi) = \tfrac{1}{2} a\rho c \Omega^2 R^2 \left\{ (x^2 \vartheta_o - \lambda x + \tfrac{1}{2} \mu^2 \vartheta_o) + \mu x \beta_o \cos \psi + (2 \mu x \vartheta_o - \lambda \mu) \sin \psi \right.$$
$$\left. - \tfrac{1}{2} \mu^2 \vartheta_o \cos 2\psi + \tfrac{1}{2} \mu^2 \beta_o \sin 2\psi \right\} \quad \ldots \quad (A.1)$$

for $0 < \psi < \pi$ and zero between $\pi < \psi < 2\pi$

or writing,

$$\left.\begin{aligned} g_o &= x^2 \vartheta_o - \lambda x + \tfrac{1}{2} \mu^2 \vartheta_o \\ g_c &= \mu x \beta_o \\ g_s &= 2 \mu x \vartheta_o - \lambda \mu \\ h_c &= - \tfrac{1}{2} \mu^2 \vartheta_o \\ h_s &= \tfrac{1}{2} \mu^2 \beta_o \end{aligned}\right\} \quad (A.2)$$

equation (A.1) becomes

$$F(\psi) = \tfrac{1}{2} a\rho c \Omega^2 R^2 \{ g_o + g_s \sin \psi + g_c \cos \psi + h_s \sin 2\psi + h_c \cos 2\psi \} \quad \ldots \quad (A.3)$$

for $0 < \psi < \pi$.

In order to obtain a harmonic series for the whole range of ψ, it can be seen that it is necessary to obtain the Fourier series for each of the terms of equation (A.3). Now function $f(\psi)$, of period 2π, can be written as

$$f(\psi) = \xi_o + \sum_{n=1}^{\infty} (\xi_{ns} \sin n\psi + \xi_{nc} \cos n\psi) \qquad (A.4)$$

where

$$\left.\begin{aligned} \xi_c &= \frac{1}{2\pi}\int_o^{2\pi} \mathbb{F}(\psi)\, d\psi \\ \xi_{ns} &= \frac{1}{\pi}\int_o^{2\pi} f(\psi) \sin n\psi\, d\psi \\ \xi_{nc} &= \frac{1}{\pi}\int_o^{2\pi} f(\psi) \cos n\psi\, d\psi \end{aligned}\right\} \qquad (A.5)$$

Thus for a function which is one between 0 and π and zero between π and 2π we have,

$$f_c(\psi) = \tfrac{1}{2} + \frac{1}{\pi}\sum_{n=1}^{\infty} \frac{1}{n}\left[1 - (-1)^n\right] \sin n\psi \qquad (A.6)$$

similarly when

$$\begin{aligned} f_{1s}(\psi) &= \sin\psi \qquad 0 < \psi < \pi \\ &= 0 \qquad \pi < \psi < 2\pi \end{aligned}$$

we have

$$f_{1s}(\psi) = \frac{1}{\pi} + \tfrac{1}{2}\sin\psi - \frac{1}{\pi}\sum_{n=2}^{\infty} \frac{1}{n^2 - 1}\left[1 + (-1)^n\right] \cos n\psi \qquad (A.7)$$

also

$$\begin{aligned} f_{1c}(\psi) &= \cos\psi \qquad 0 < \psi < \pi \\ &= 0 \qquad \pi < \psi < 2\pi \end{aligned}$$

becomes

$$f_{1c}(\psi) = \tfrac{1}{2}\cos\psi + \frac{1}{\pi}\sum_{n=2}^{\infty}\frac{n}{n^2-1}\left[1+(-1)^n\right]\sin n\psi \qquad (A.8)$$

and

$$\begin{aligned} f_{2s}(\psi) &= \sin 2\psi \qquad 0 < \psi < \pi \\ &= 0 \qquad\qquad \pi < \psi < 2\pi \end{aligned}$$

becomes

$$f_{2s}(\psi) = \frac{4}{3\pi}\cos\psi + \tfrac{1}{2}\sin 2\psi - \frac{1}{\pi}\sum_{n=3}^{\infty}\frac{2}{n^2-4}\left[1-(-1)^n\right]\cos n\psi \qquad (A.9)$$

and

$$\begin{aligned} f_{2c}(\psi) &= \cos 2\psi \qquad 0 < \psi < \pi \\ &= 0 \qquad\qquad \pi < \psi < 2\pi \end{aligned}$$

becomes

$$f_{2c}(\psi) = -\frac{2}{3\pi}\sin\psi + \tfrac{1}{2}\cos 2\psi + \frac{1}{\pi}\sum_{n=3}^{\infty}\frac{n}{n^2-4}\left[1-(-1)^n\right]\sin n\psi \qquad (A.10)$$

Thus the compoents $b_n(x)$ and $a_n(x)$ of equation (8) are given by equations (9), (A.3) and (A.6) - (A.10) i.e.

$$
\left.
\begin{aligned}
b_o(x) &= JR\left\{\frac{g_o}{2} + \frac{g_s}{\pi}\right\} \\
b_1(x) &= JR\left\{\frac{g_c}{2} + h_s\,\frac{4}{3\pi}\right\} \\
b_2(x) &= JR\left\{-\frac{2g_s}{3\pi} + \frac{h_c}{2}\right\} \\
a_1(x) &= JR\left\{\frac{g_s}{2} + \frac{2g_o}{\pi} - \frac{2}{3\pi}\,h_c\right\} \\
a_2(x) &= JR\left\{\frac{4g_c}{3\pi} + \frac{h_s}{2}\right\}
\end{aligned}
\right\} \qquad (A.11)
$$

and in general for $n \geq 3$

$$
b_n(x) = JR\left\{-\frac{g_s}{\pi}\left(\frac{1}{n^2-1}\right)\left[1+(-1)^n\right] - \frac{h_s}{\pi}\,\frac{2}{n^2-4}\left[1-(-1)^n\right]\right\} \qquad (A.12)
$$

$$
a_n(x) = JR\left\{\frac{g_o}{\pi}\,\frac{1}{n}\left[1-(-1)^n\right] + \frac{g_c}{\pi}\left(\frac{n}{n^2-1}\right)\left[1+(-1)^n\right] + \frac{h_c}{\pi}\,\frac{n}{n^2-4}\left(1-(-1)^n\right)\right\}
$$

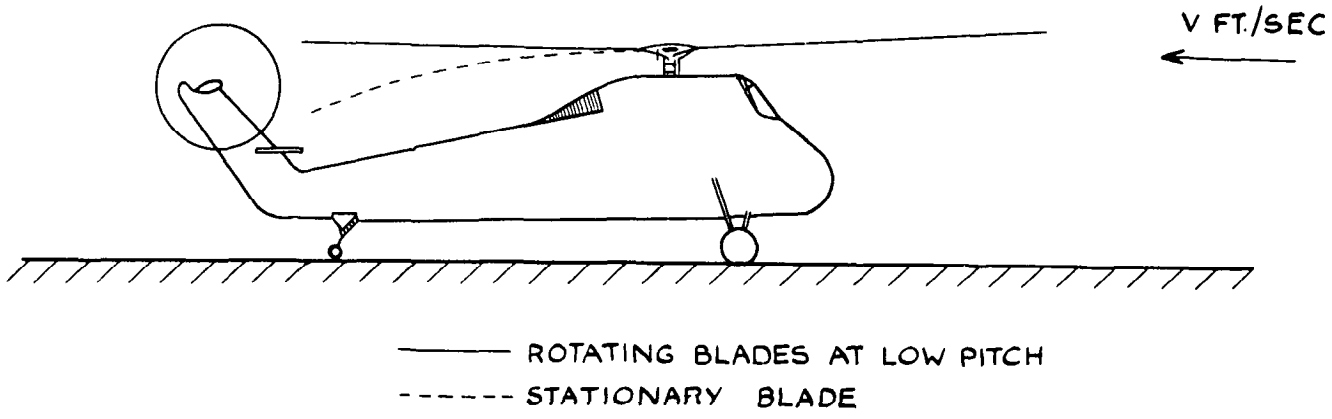

FIG. 1. A TYPICAL HELICOPTER ON THE GROUND IN A WIND.

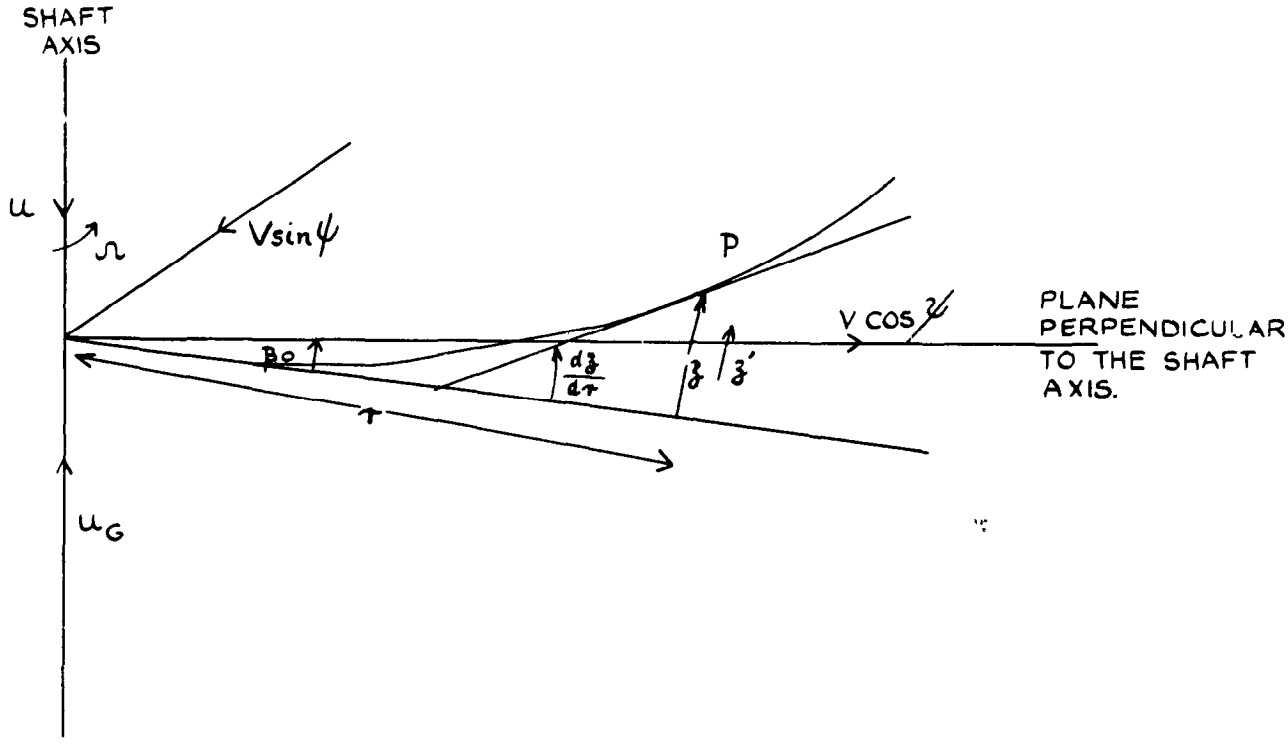

FIG. 2. DIAGRAM SHOWING THE VELOCITIES AT AZIMUTH ANGLE ψ.

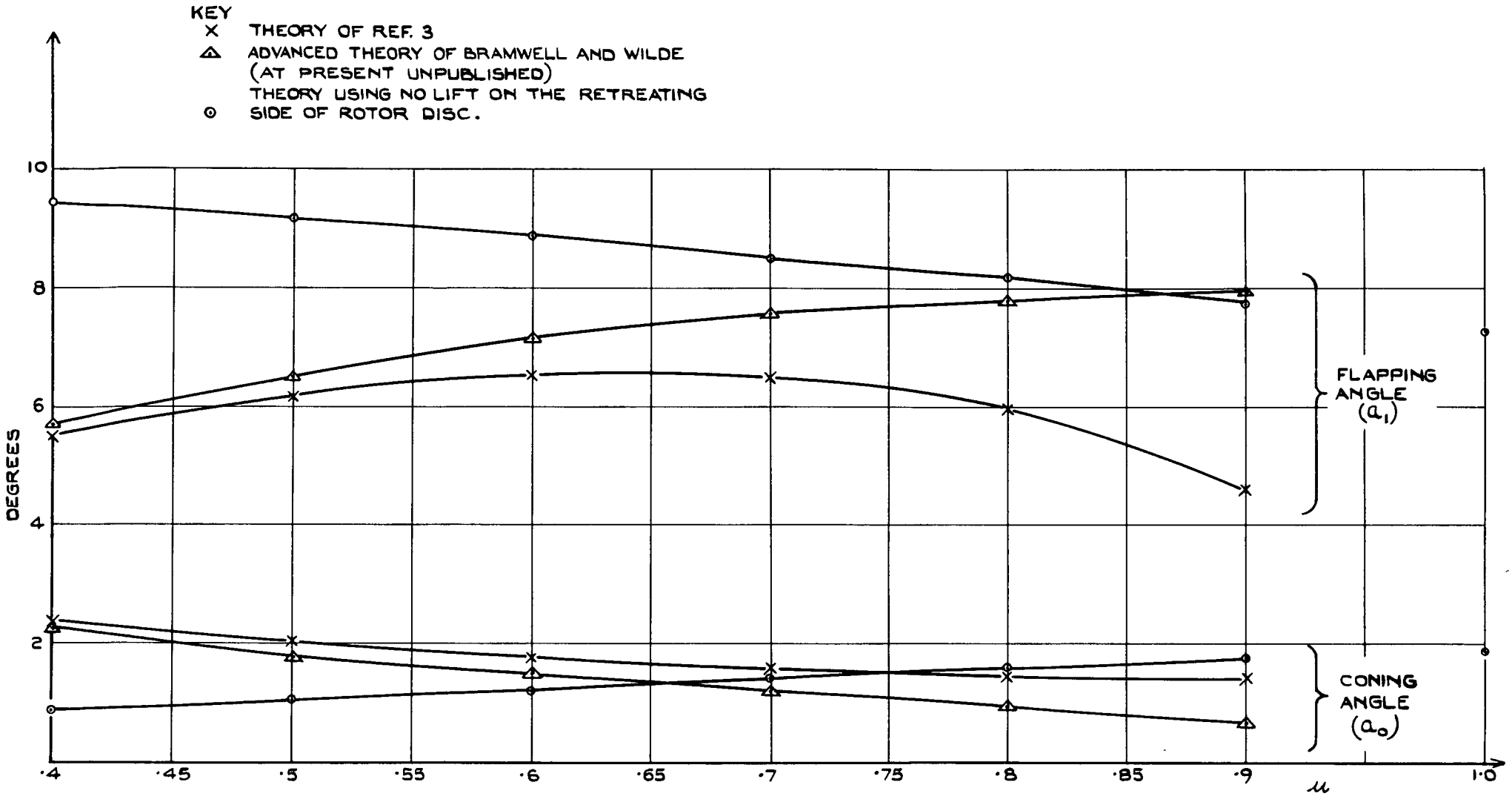

FIG. 3. COMPARISON BETWEEN FLAPPING THEORIES.

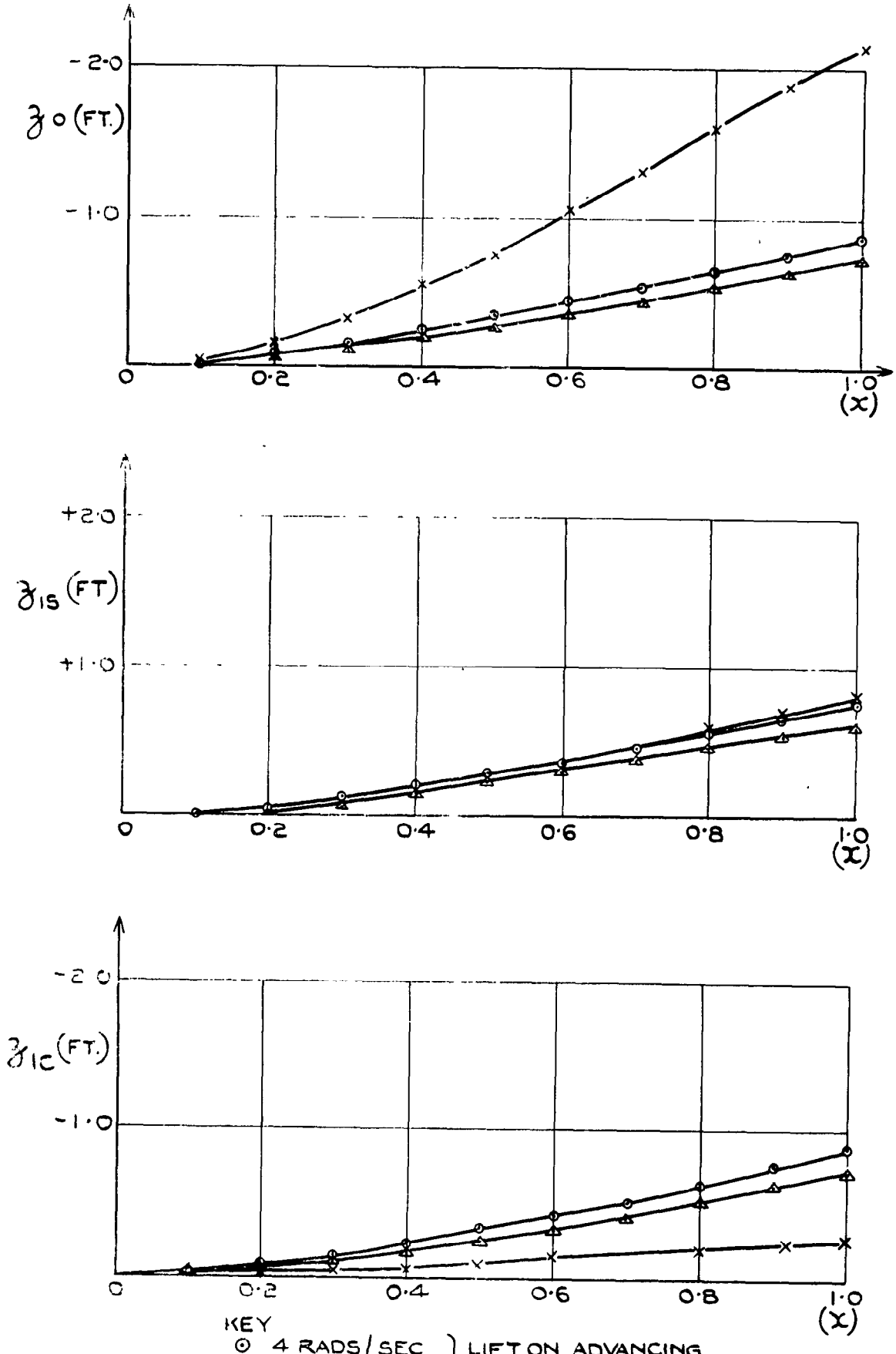

FIG. 4. BLADE DEFLECTION HARMONICS FOR WHIRLWIND HELICOPTER IN 30 KT. WIND ON THE GROUND (NO CYCLIC CONTROL)

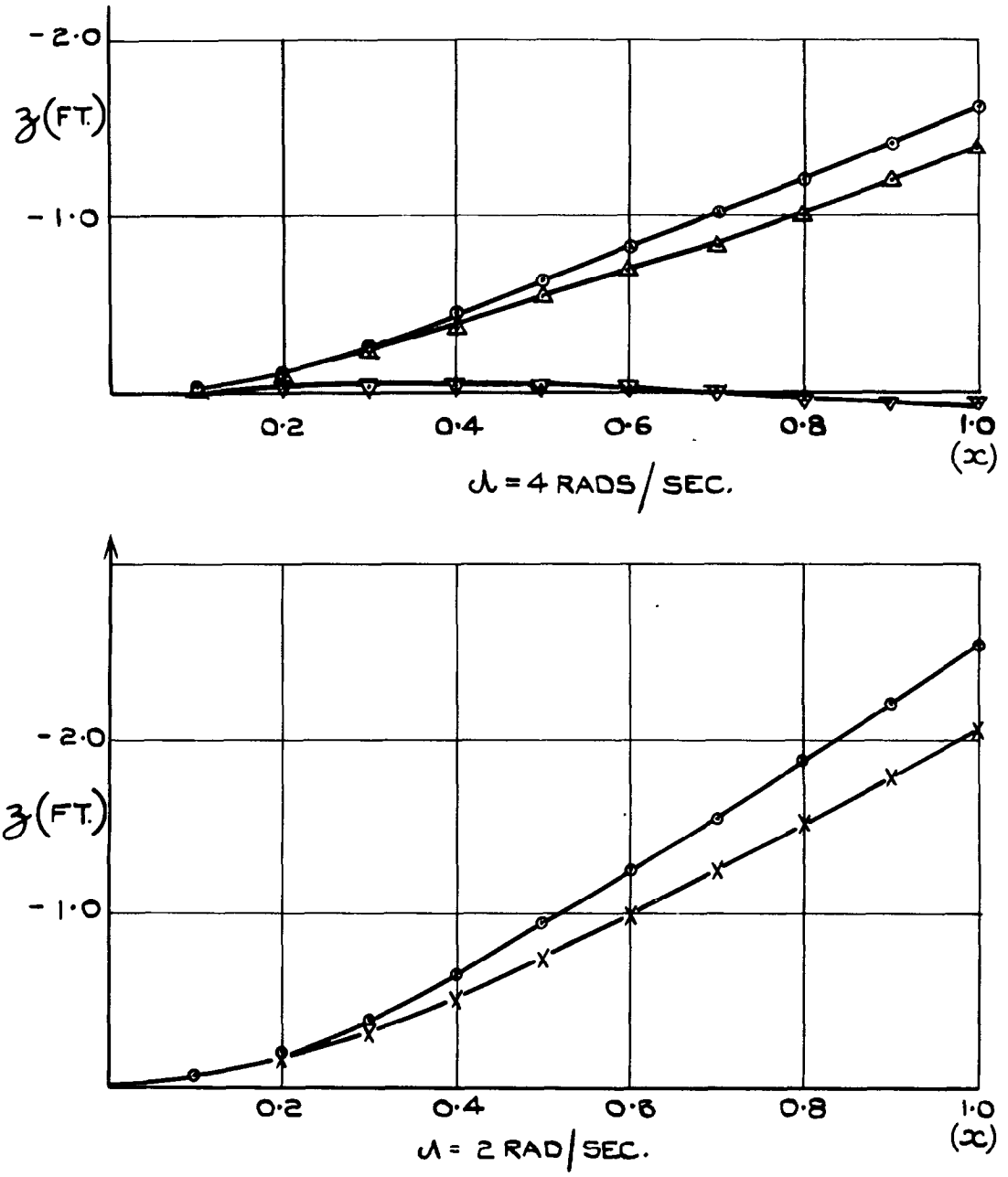

FIG. 5. FORE AND AFT BLADE DEFLECTIONS FOR WHIRLWIND HELICOPTER IN A 30 KT. WIND ON THE GROUND (NO CYCLIC CONTROL)

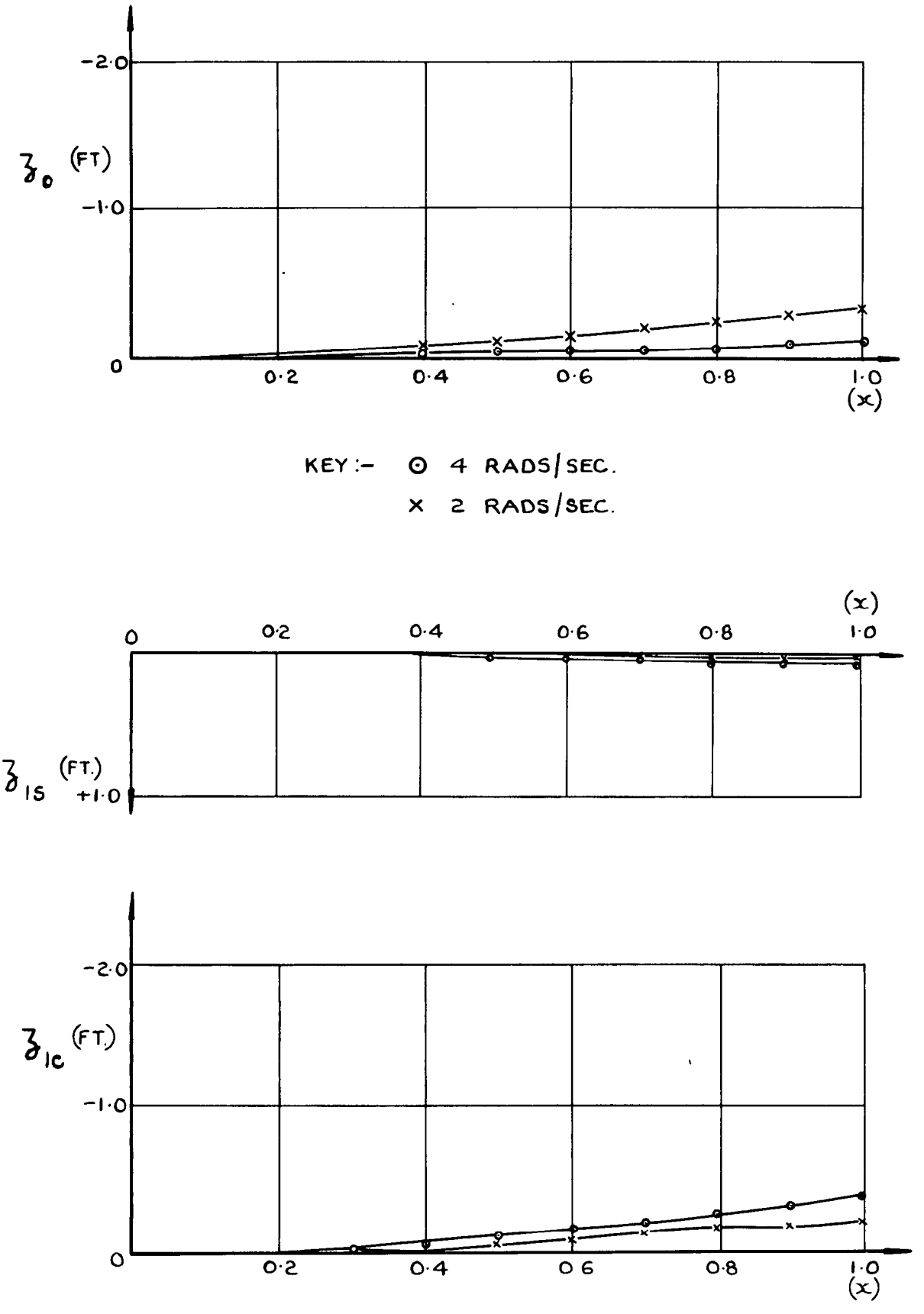

FIG. 6. BLADE DEFLECTIONS HARMONICS FOR P531 HELICOPTER IN 25KT WIND ON THE GROUND. (NO CYCLIC CONTROL.)

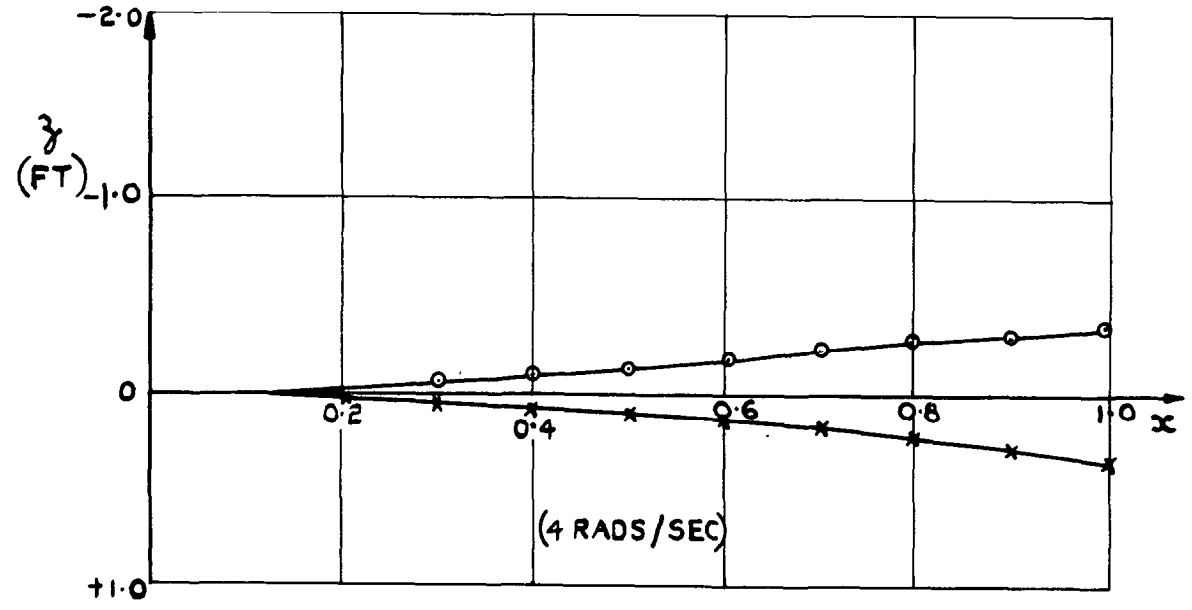

KEY

⊙ $\psi = 0°$

X $\psi = 180°$

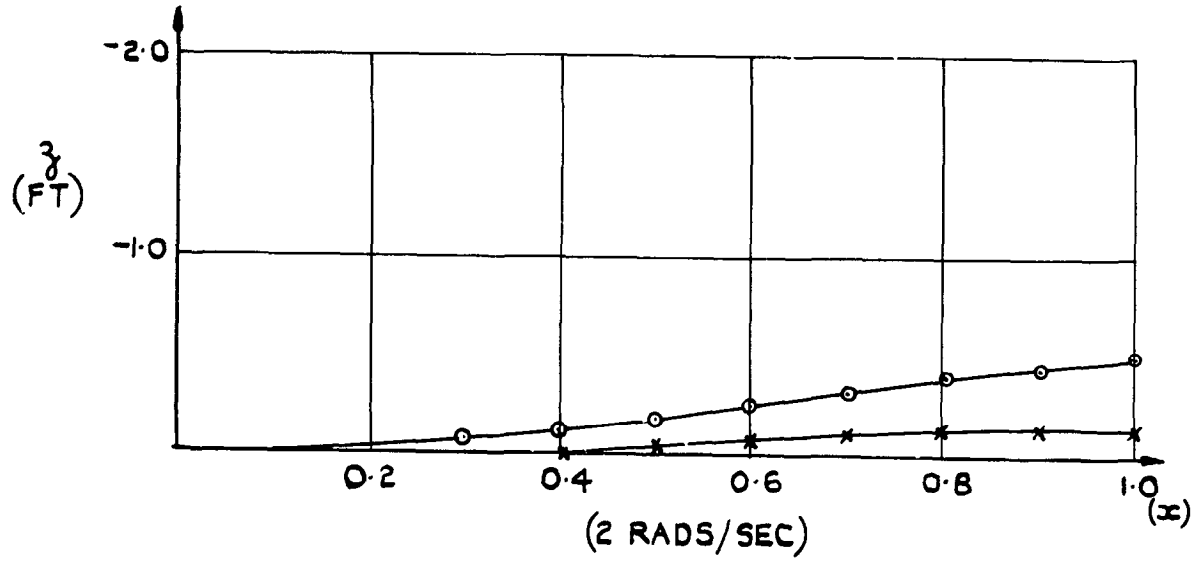

FIG. 7. FORE & AFT BLADE DEFLECTIONS FOR P531 HELICOPTER IN 25 KT. WIND ON THE GROUND (NO CYCLIC CONTROL)

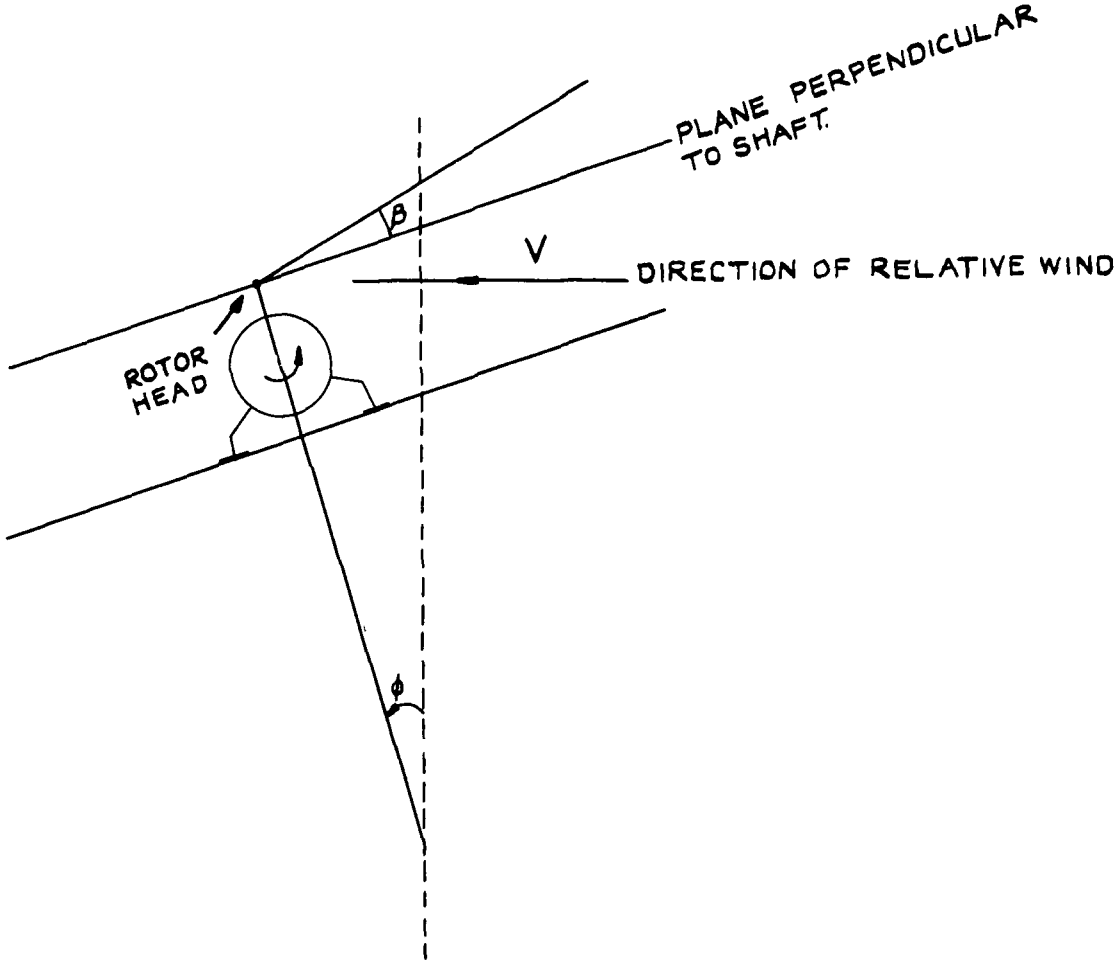

FIG. 8. DIAGRAM SHOWING HELICOPTER ATTACHED TO A ROLLING SHIP IN A SIDE WIND.

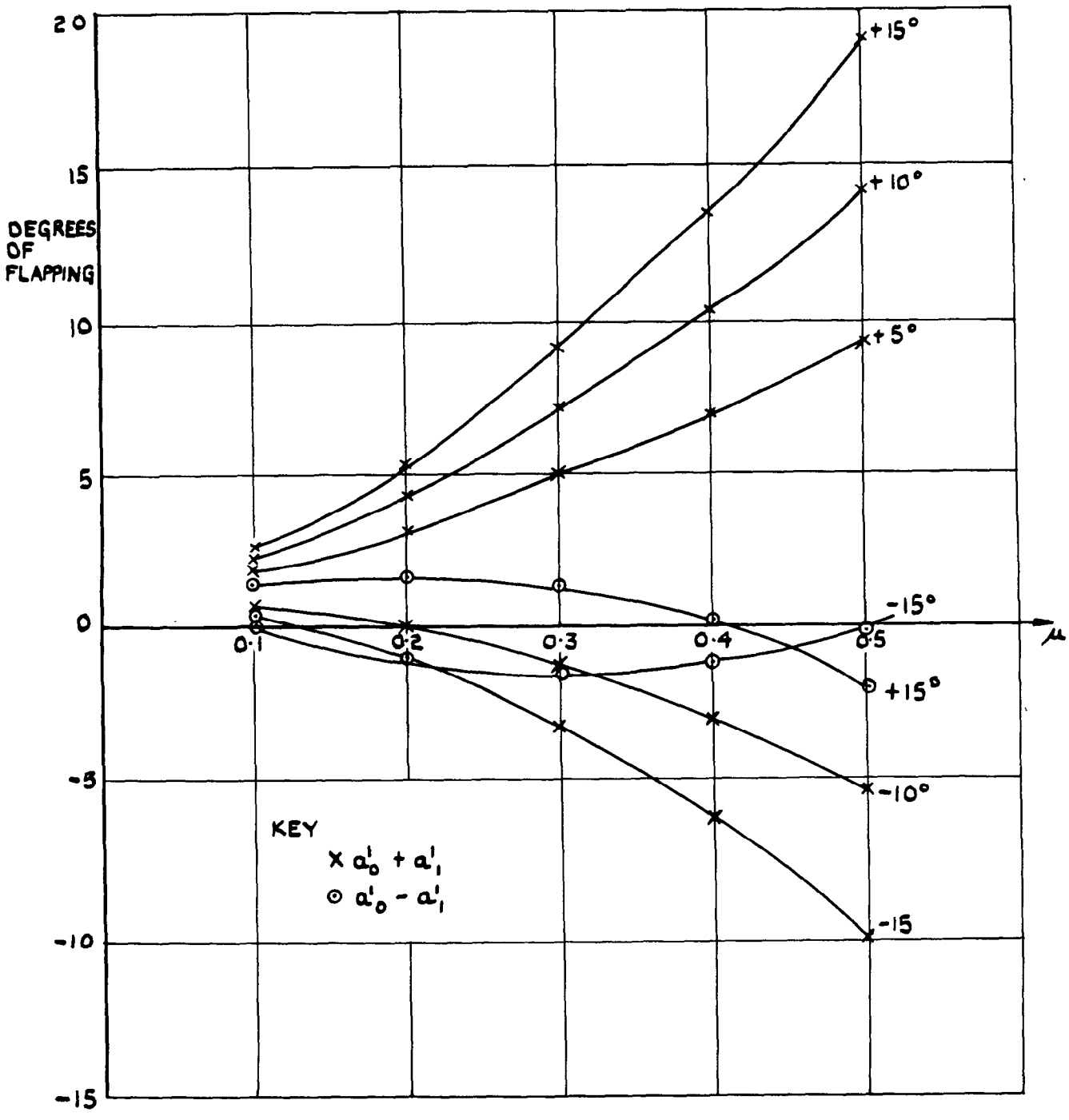

FIG. 9. (a) VARIATION OF THE FLAPPING ANGLE WITH μ FOR SEVERAL ROLL ANGLES (P531 HELICOPTER).

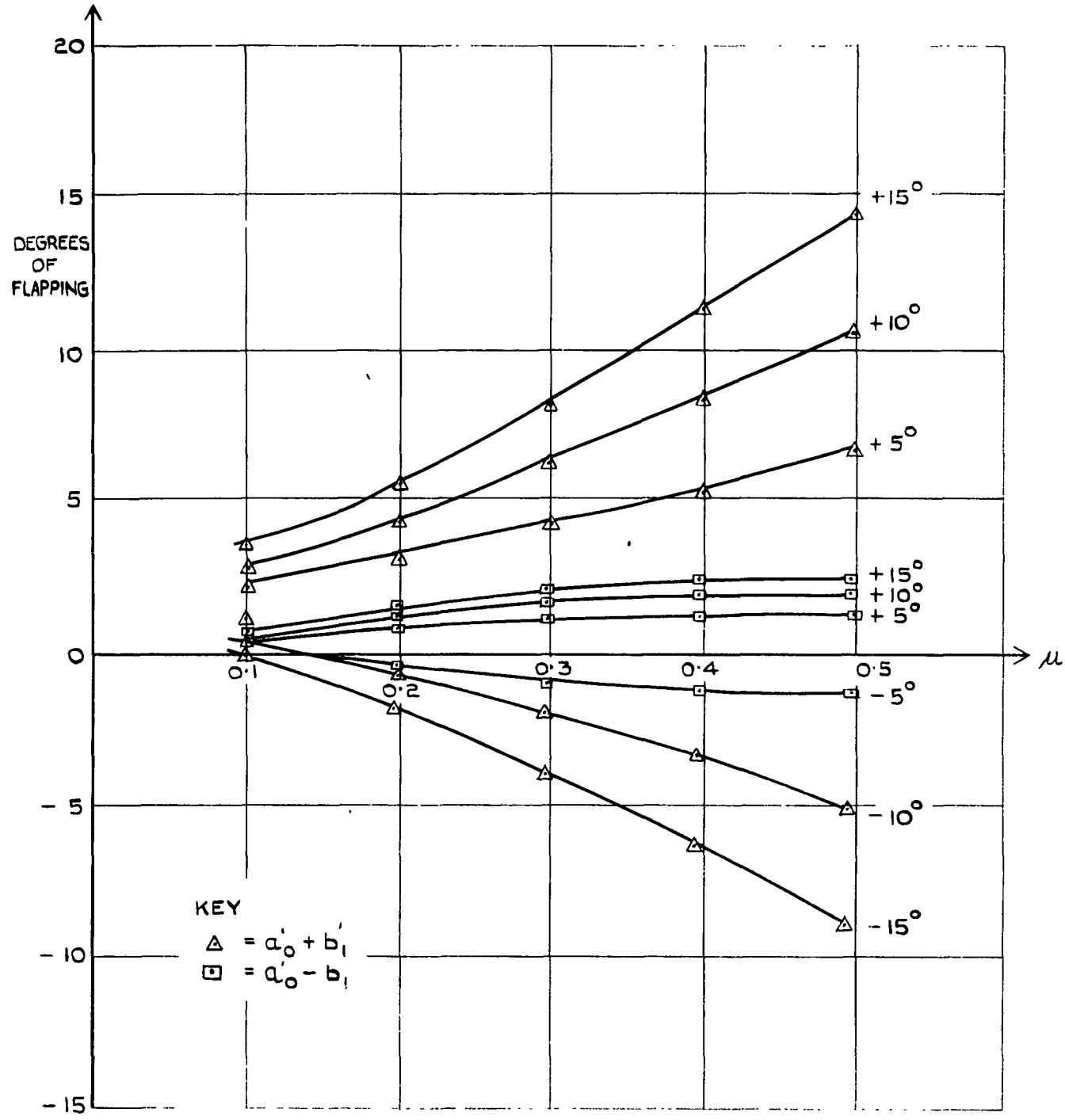

FIG. 9.(b) VARIATION OF THE FLAPPING ANGLE WITH μ FOR SEVERAL ROLL ANGLES (P. 531 HELICOPTER)

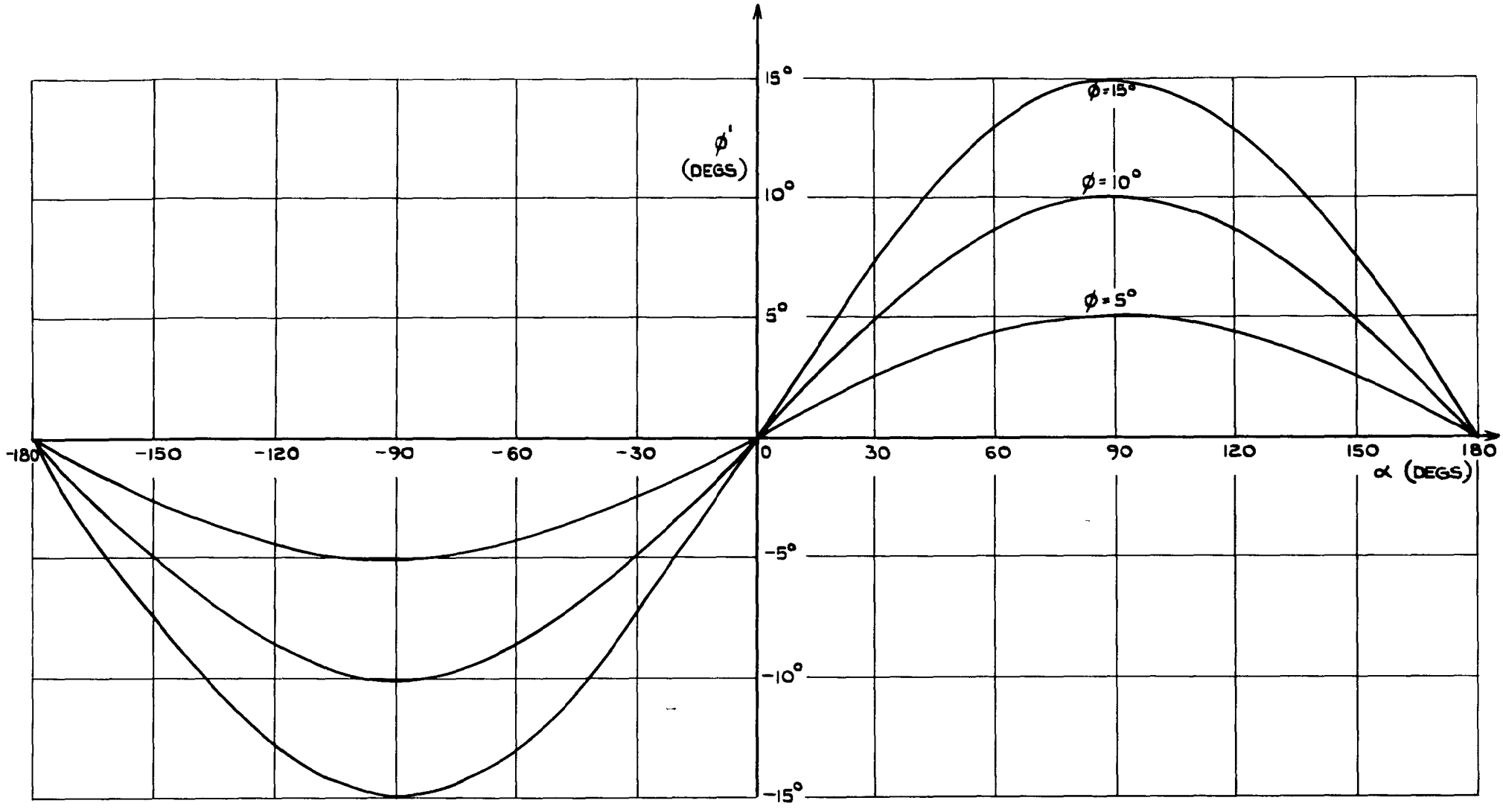

FIG. 10. VARIATION OF ϕ' WITH α

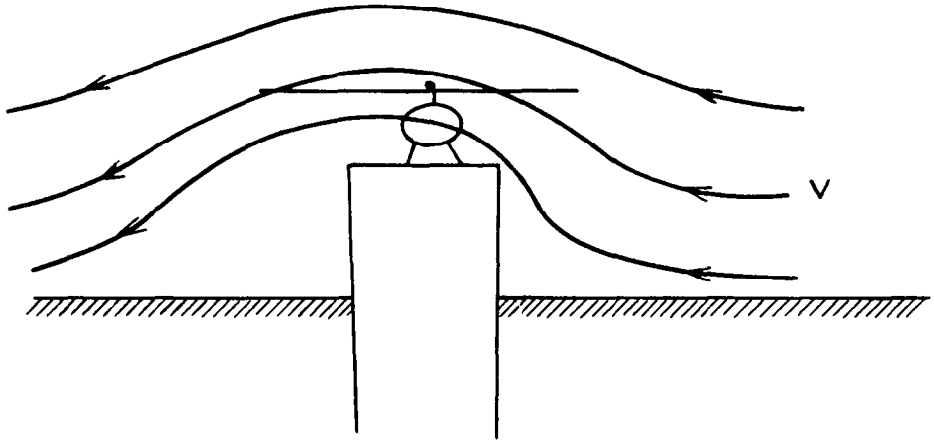

FIG. 11. DIAGRAM SHOWING THE DISTURBED AIRFLOW THROUGH THE ROTOR DISC DUE TO THE PRESENCE OF THE SHIP

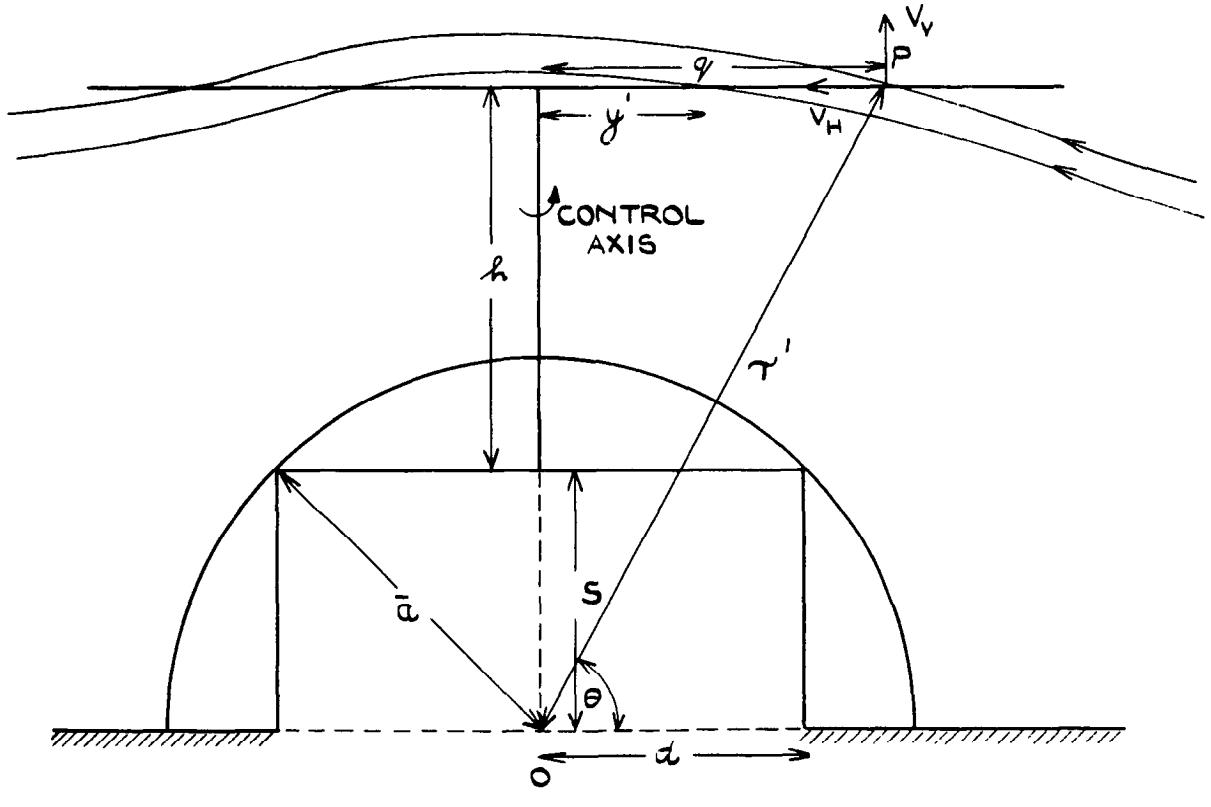

FIG. 12 DIAGRAM SHOWING THE DECK AND THE EQUIVALENT TWO DIMENSIONAL CIRCULAR CYLINDER

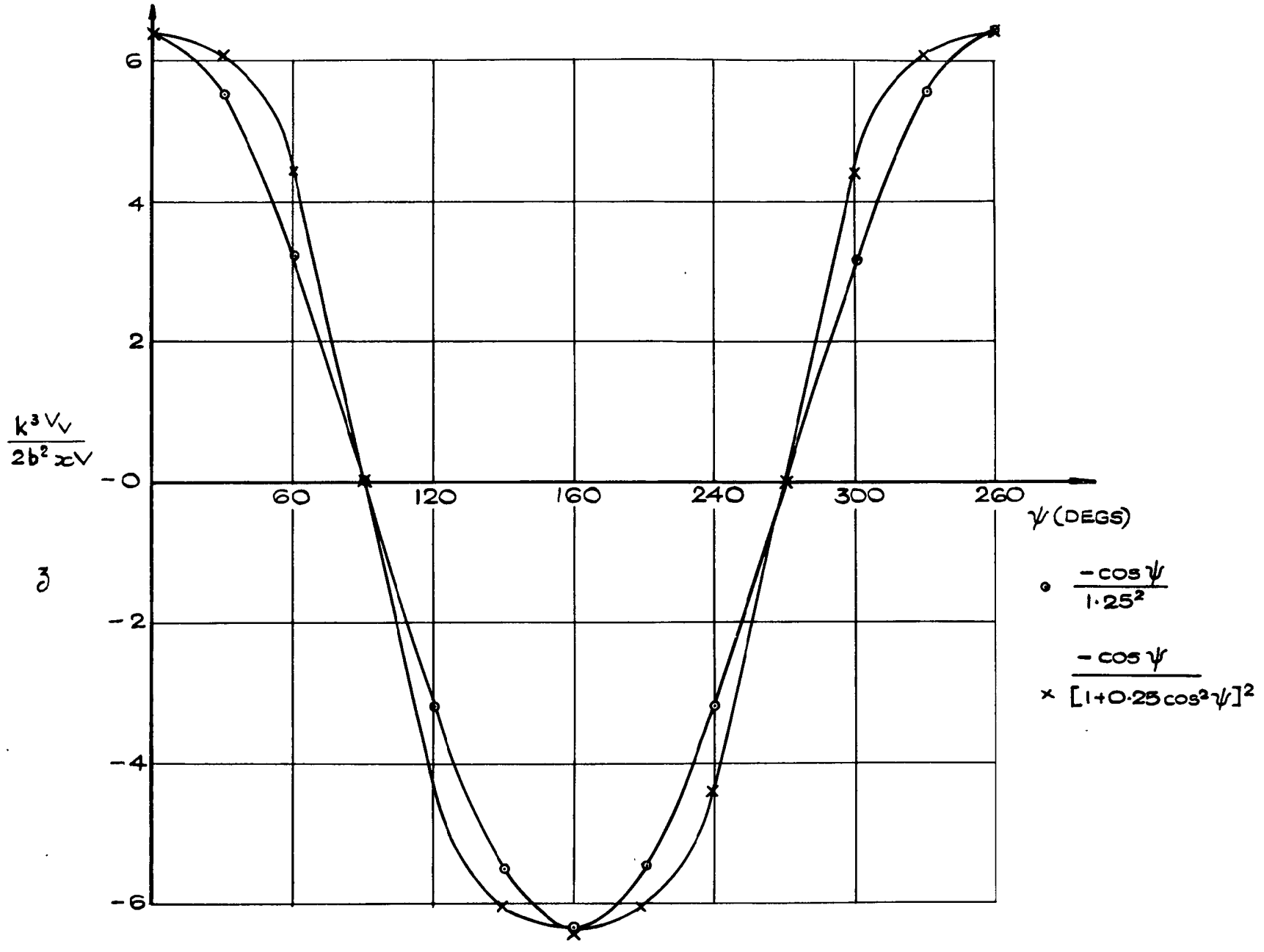

FIG.13. VARIATION OF $\frac{k^3 V_v}{2b^2 x V}$ WITH ψ.

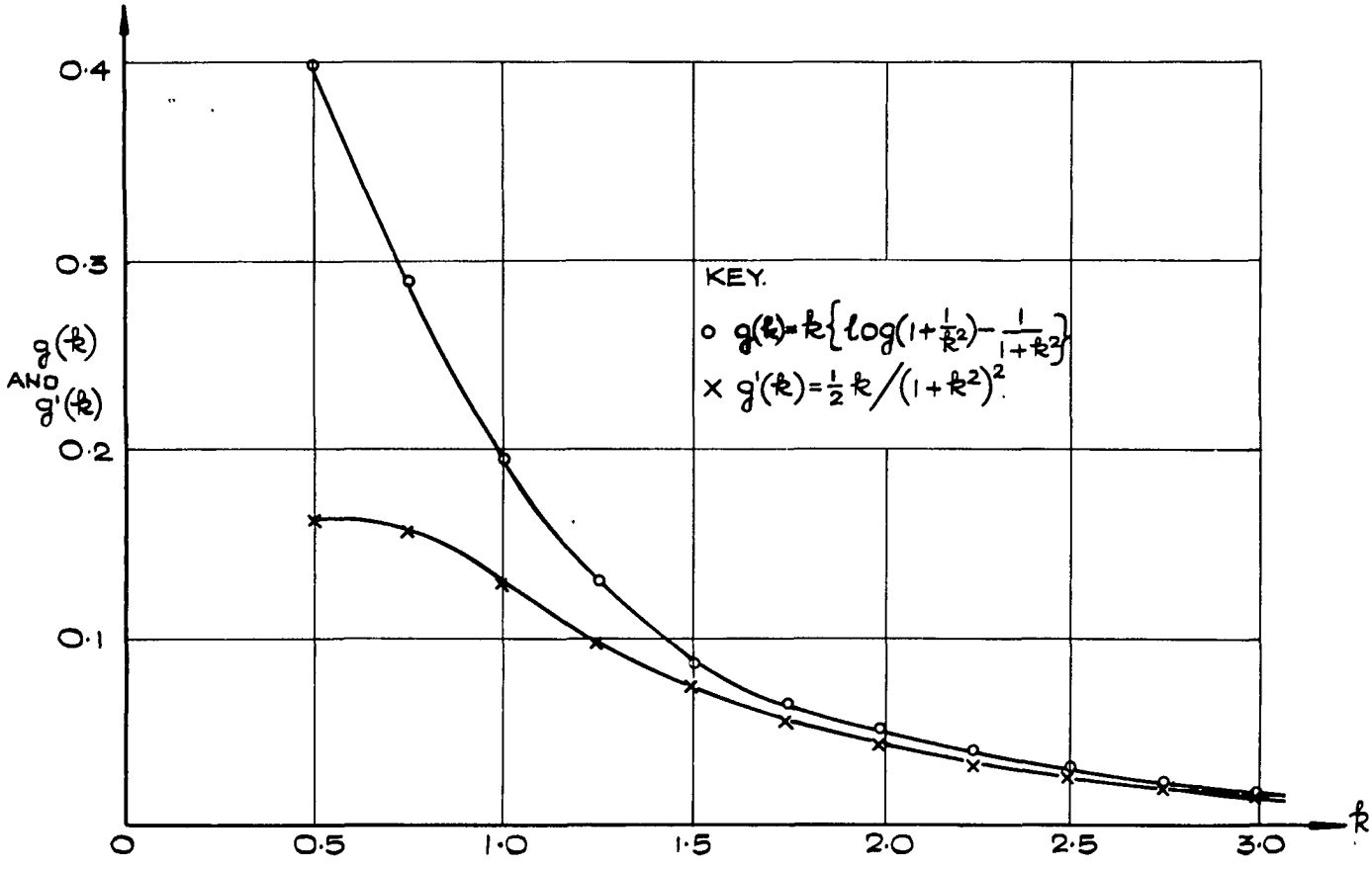

FIG.14. VARIATION OF g(k) AND g'(k) WITH k.

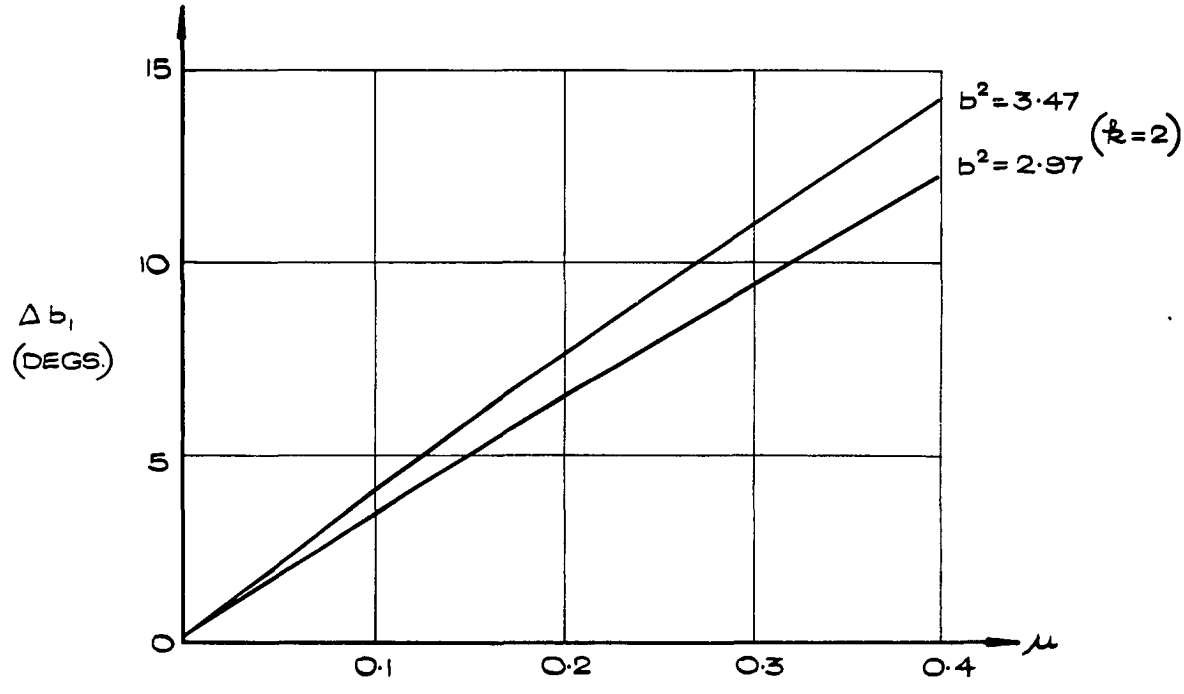

FIG.15. THE INCREMENT TO b_1 DUE TO THE PRESENCE OF THE SHIP.

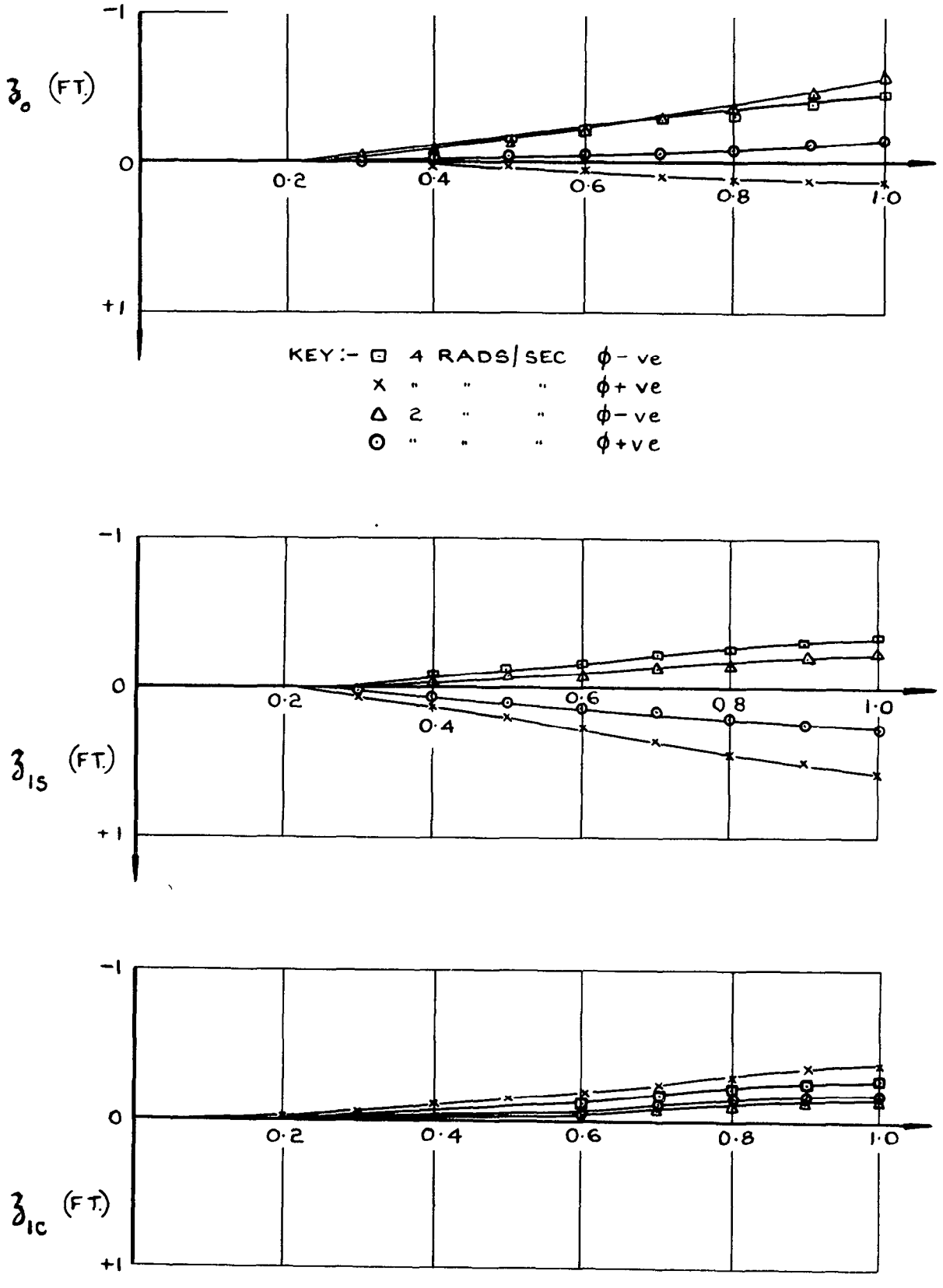

FIG. 16. BLADE DEFLECTION HARMONICS FOR THE P531 HELICOPTER IN A 25KT. WIND ON A FRIGATE WITH 15° ROLL (NO CYCLIC CONTROL)

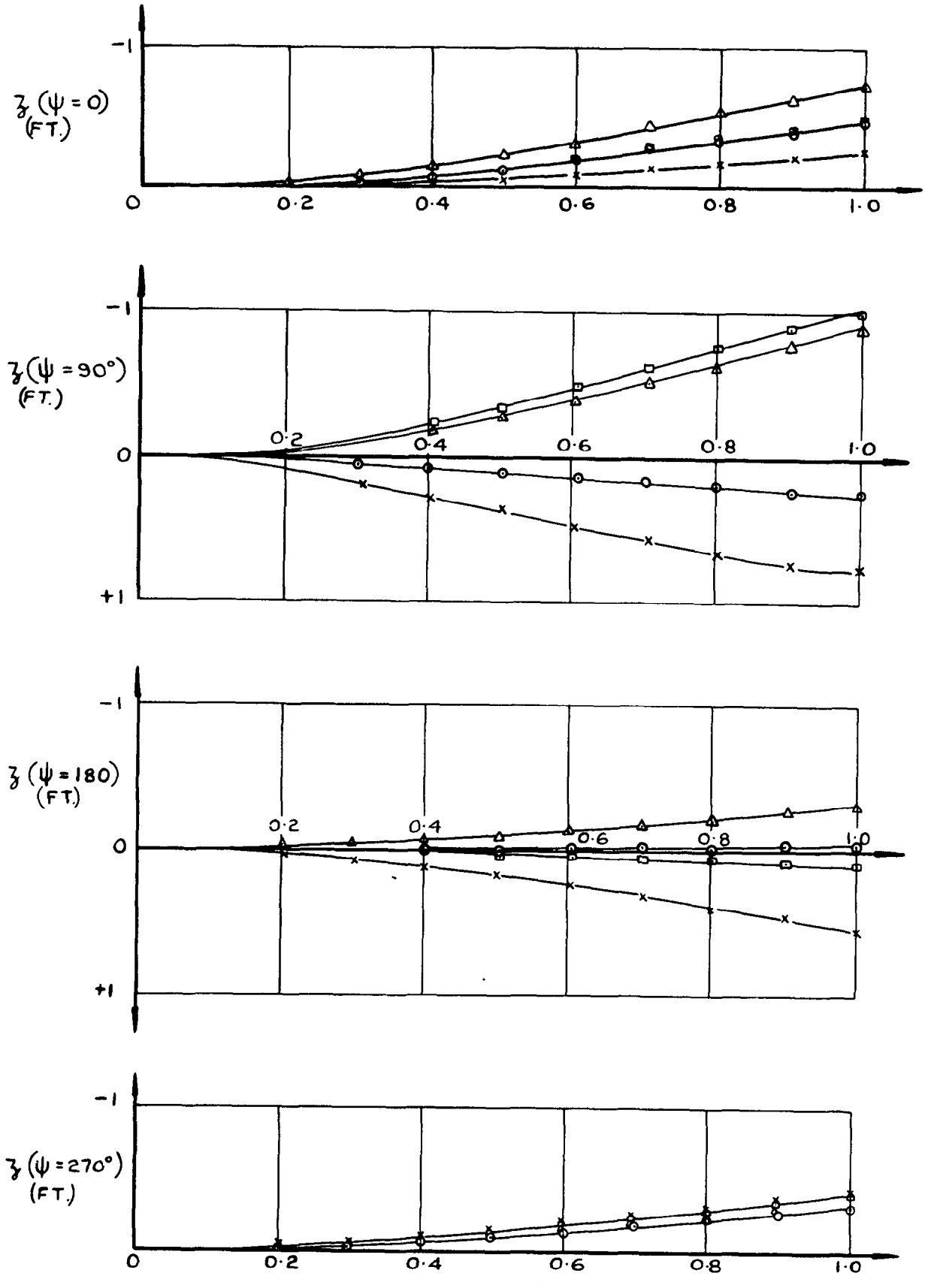

FIG. 17. TOTAL BLADE DEFLECTIONS FOR P531 HELICOPTER IN A 25KT WIND ON A FRIGATE WITH 15° ROLL. (NO CYCLIC CONTROL.)

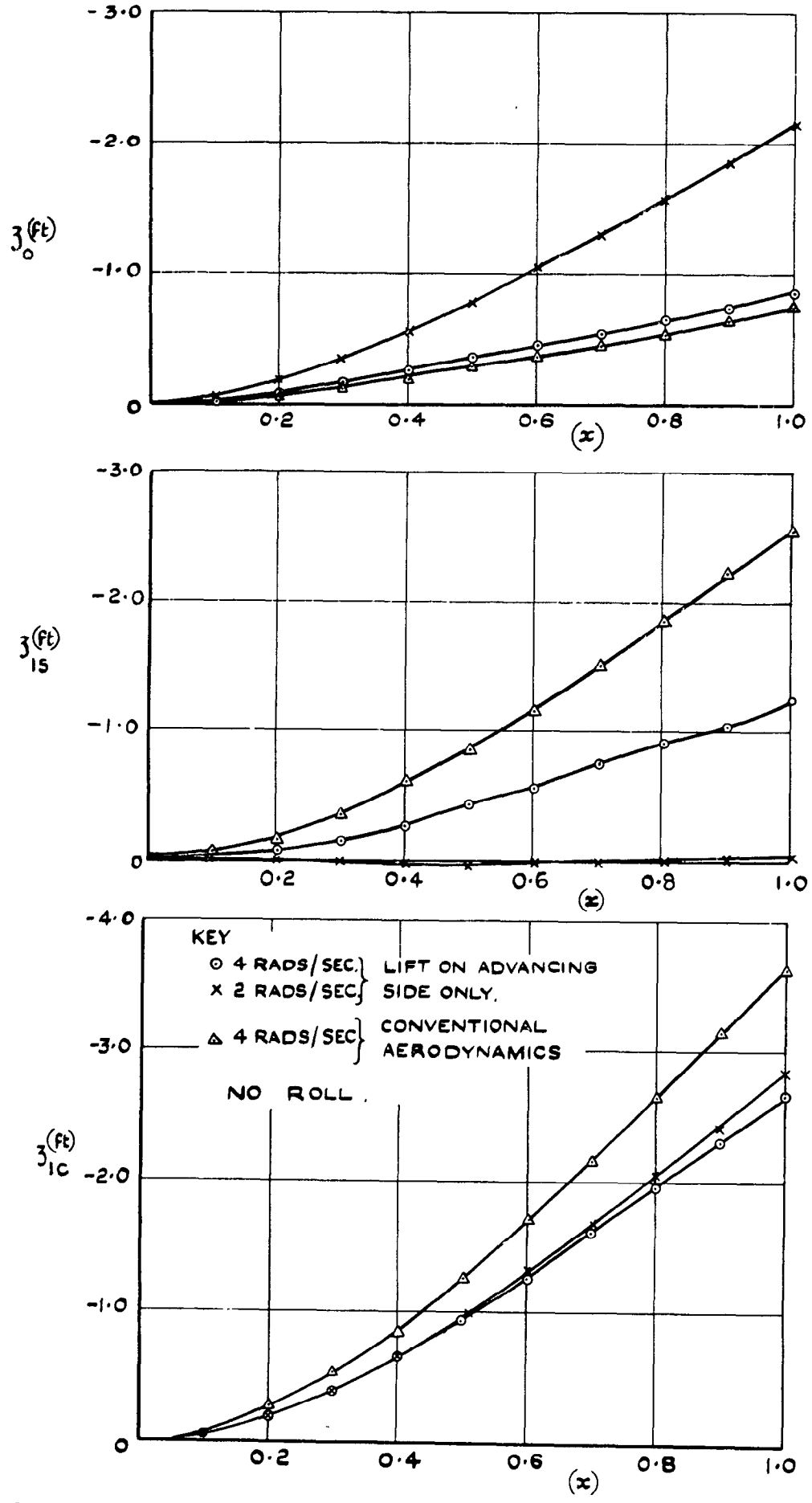

FIG. 18. BLADE DEFLECTION HARMONICS FOR WHIRLWIND HELICOPTER ABOARD A FRIGATE IN A SIDE WIND OF 30 KTS - NO CYCLIC CONTROL.

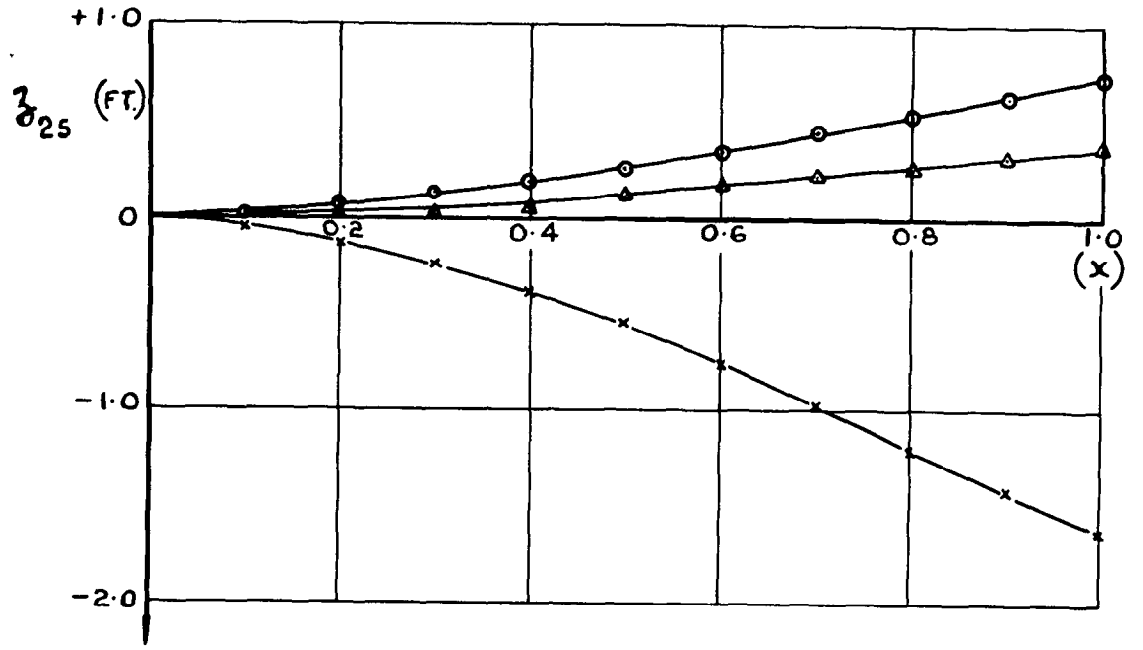

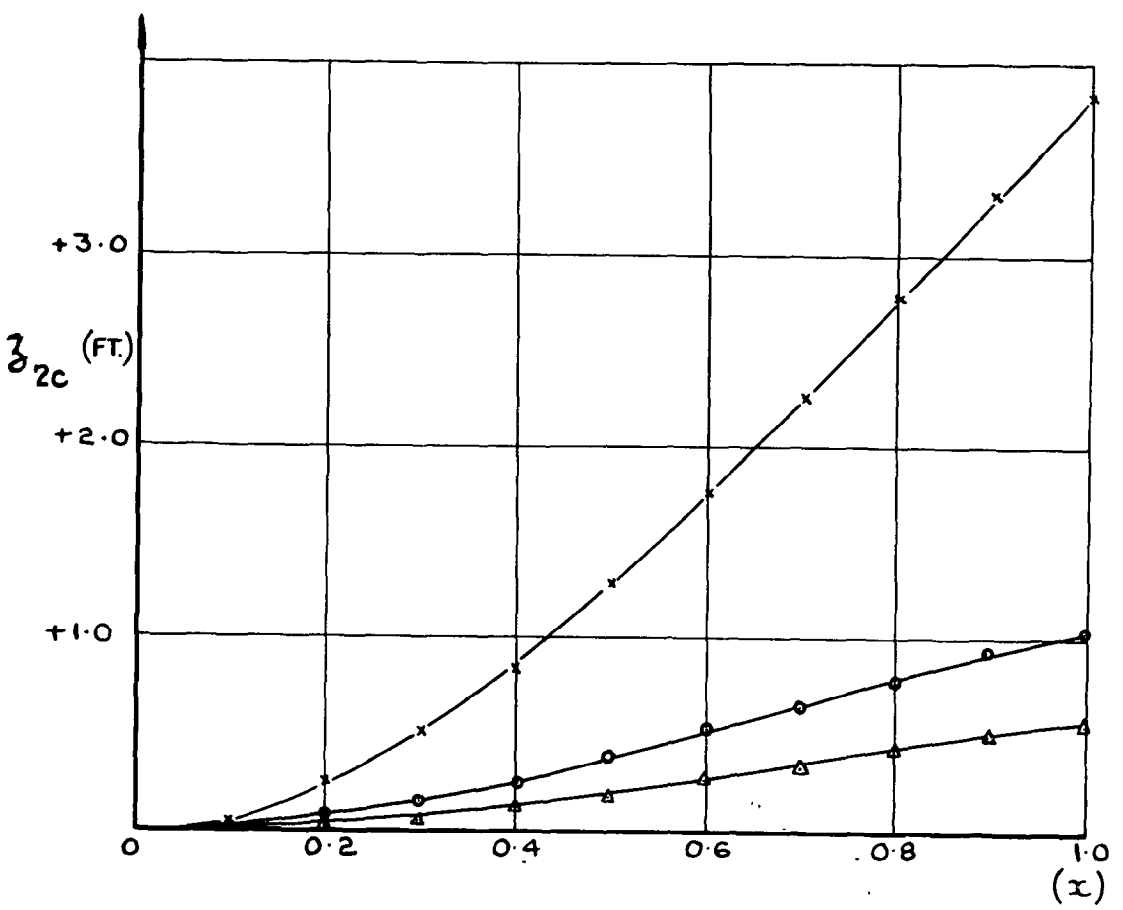

FIG. 18 (CONT.)

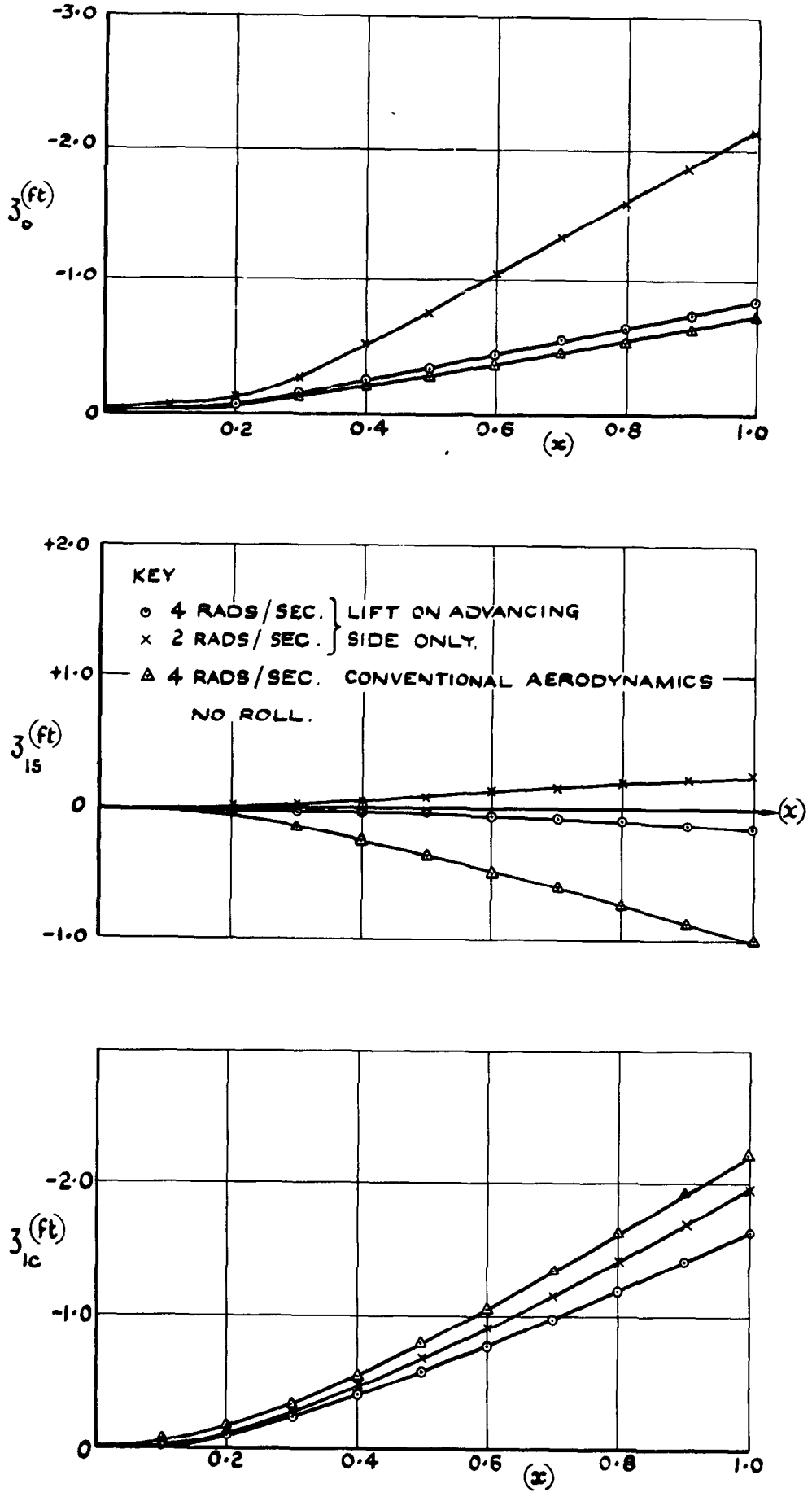

FIG.19. BLADE DEFLECTION HARMONICS FOR WHIRLWIND HELICOPTER ABOARD A FRIGATE IN A SIDE WIND OF 30 KTS $-A_1 = -5°$.

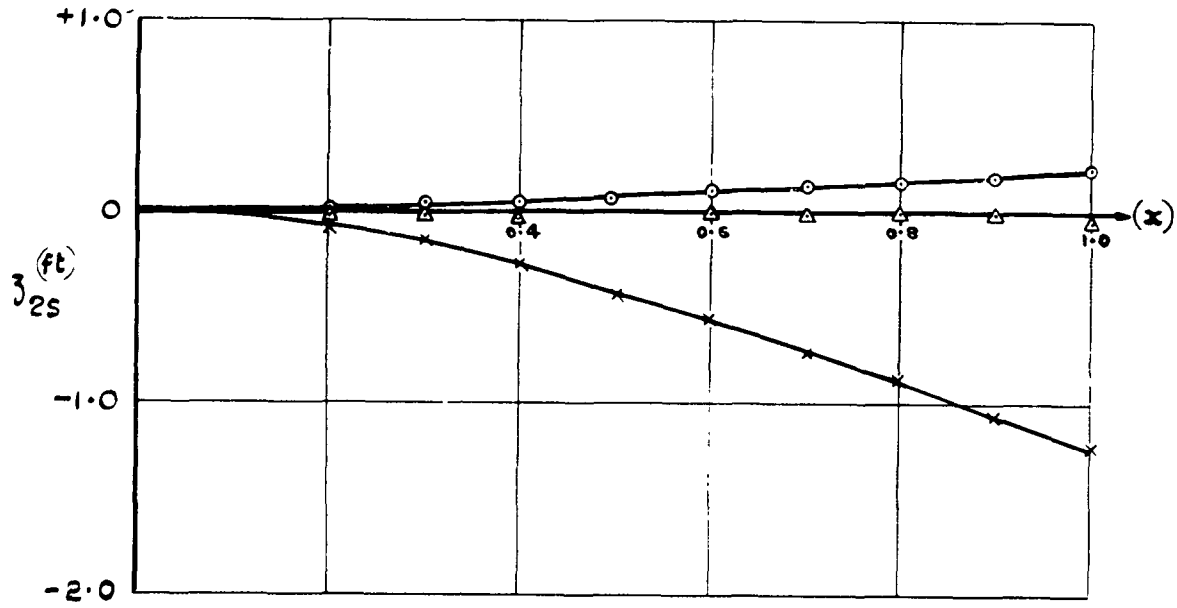

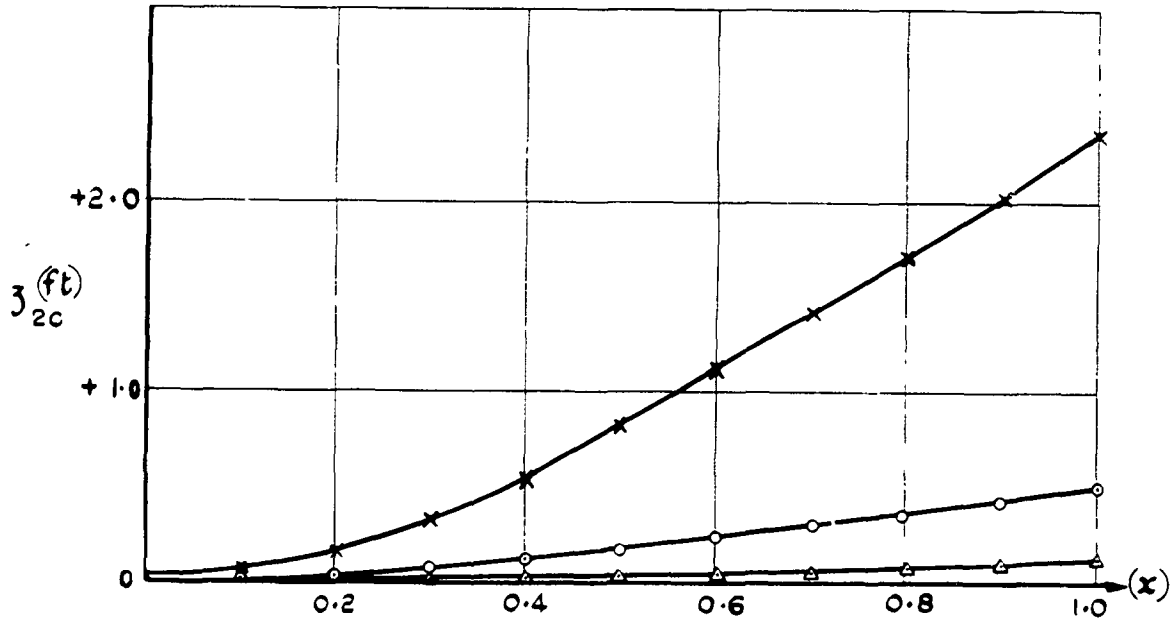

FIG. 19 (contd.)

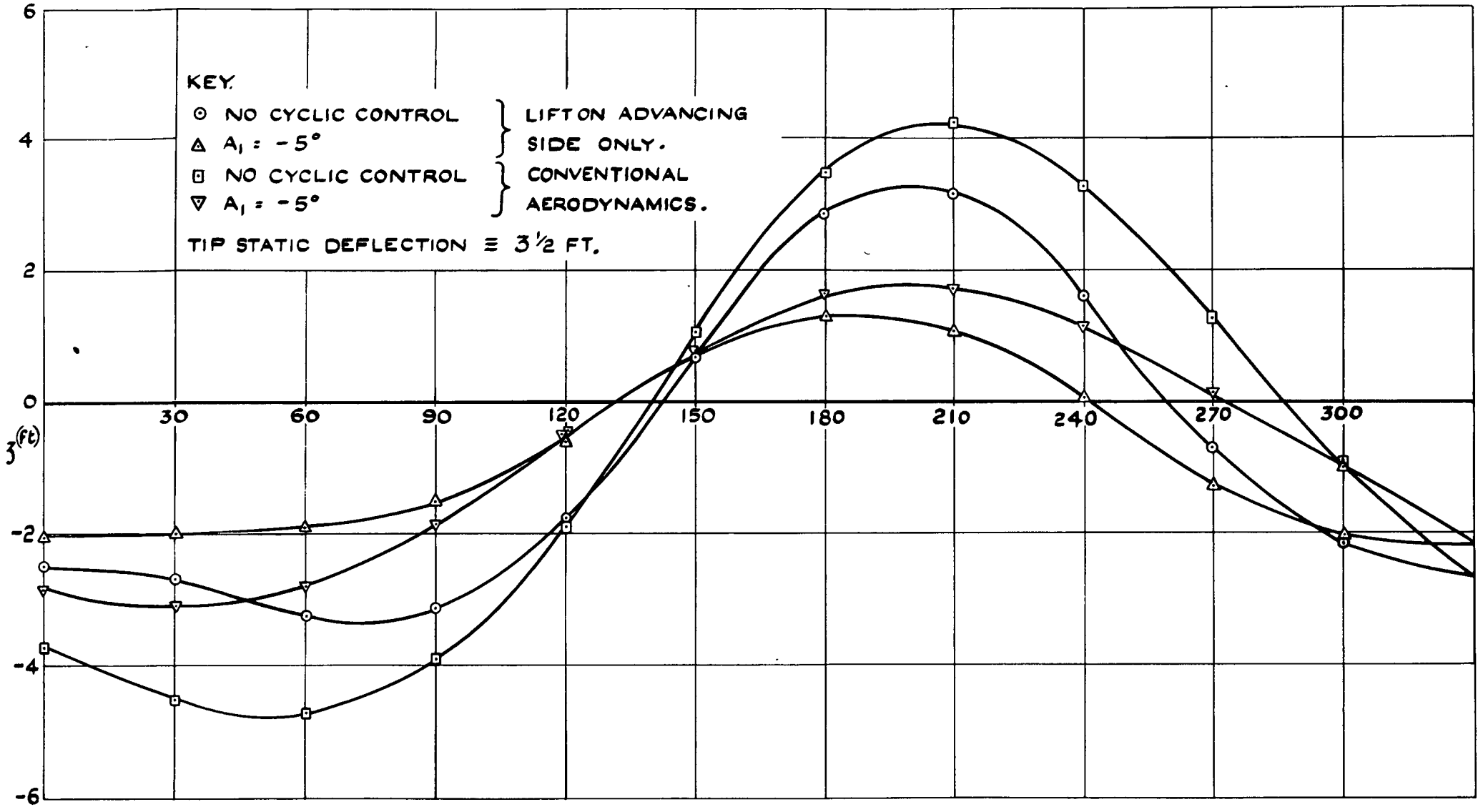

FIG 20(a) VARIATION OF TIP DEFLECTION WITH AZIMUTH FOR WHIRLWIND ON FRIGATE IN 30 KT WIND (4 rads/sec.)

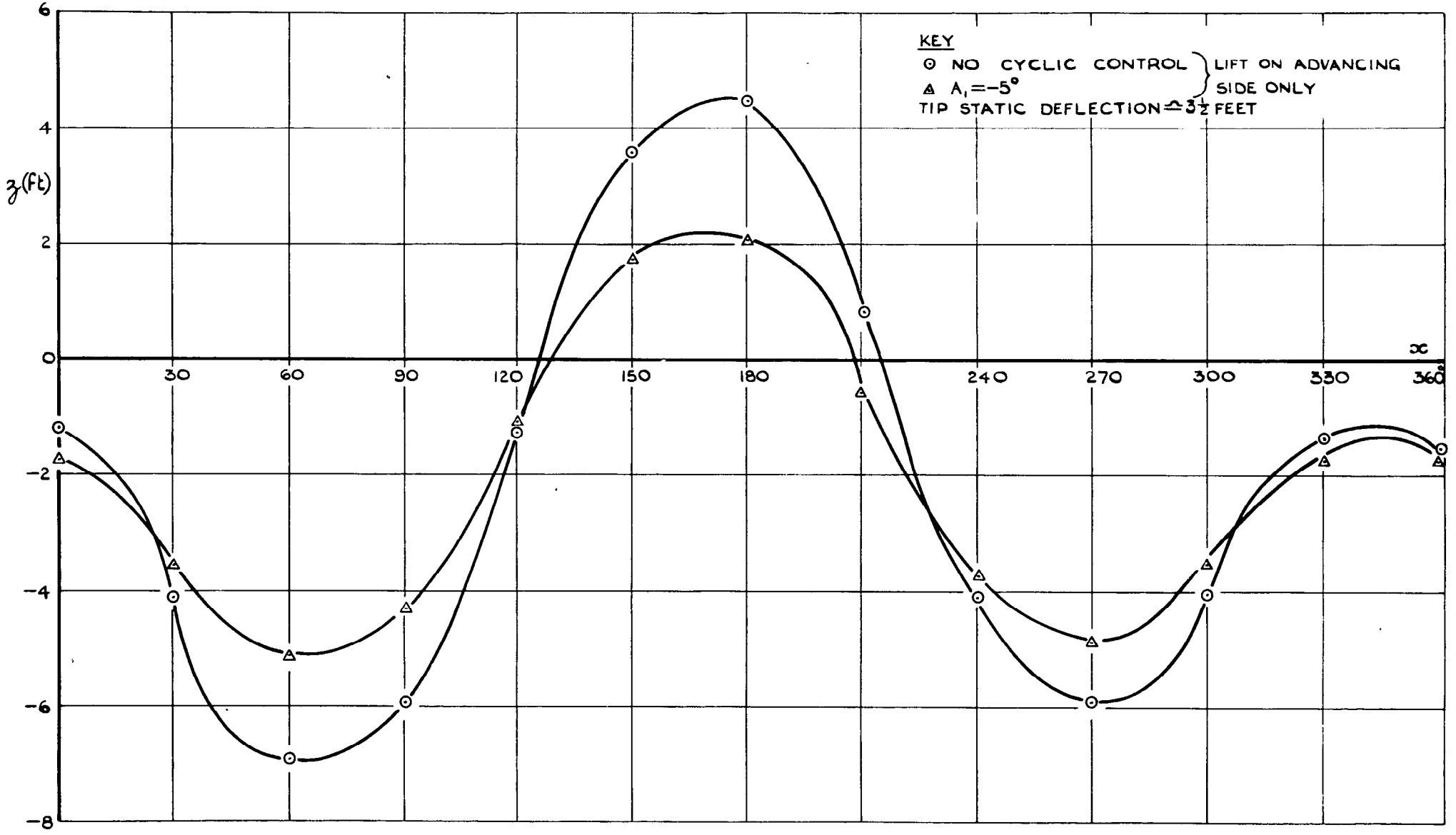

FIG. 20(b) VARIATION OF TIP DEFLECTION WITH AZIMUTH FOR WHIRLWIND ON FRIGATE IN 30KT. WIND. (2 rads./sec.)

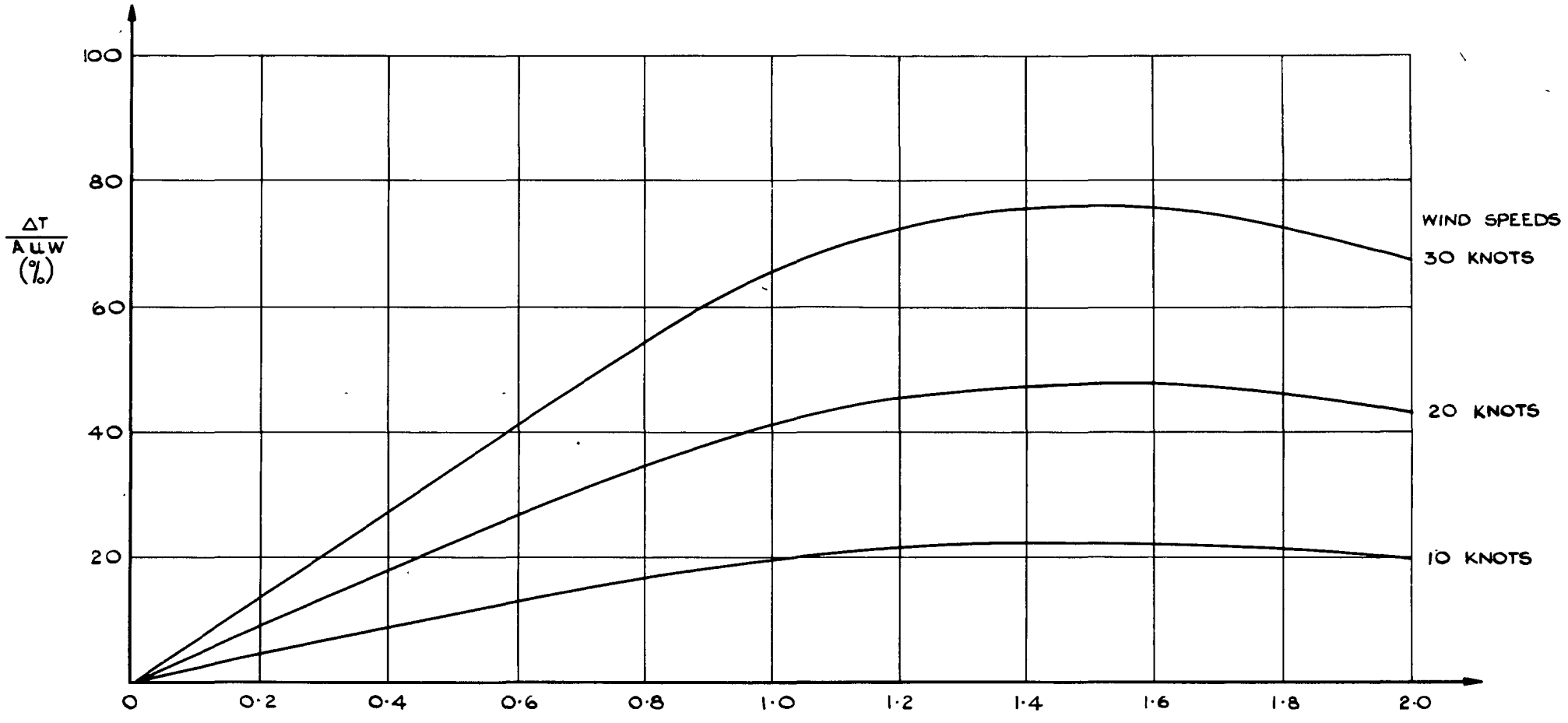

FIG.21. THE INCREASE IN LIFT DUE TO THE CLIFF EDGE EFFECT

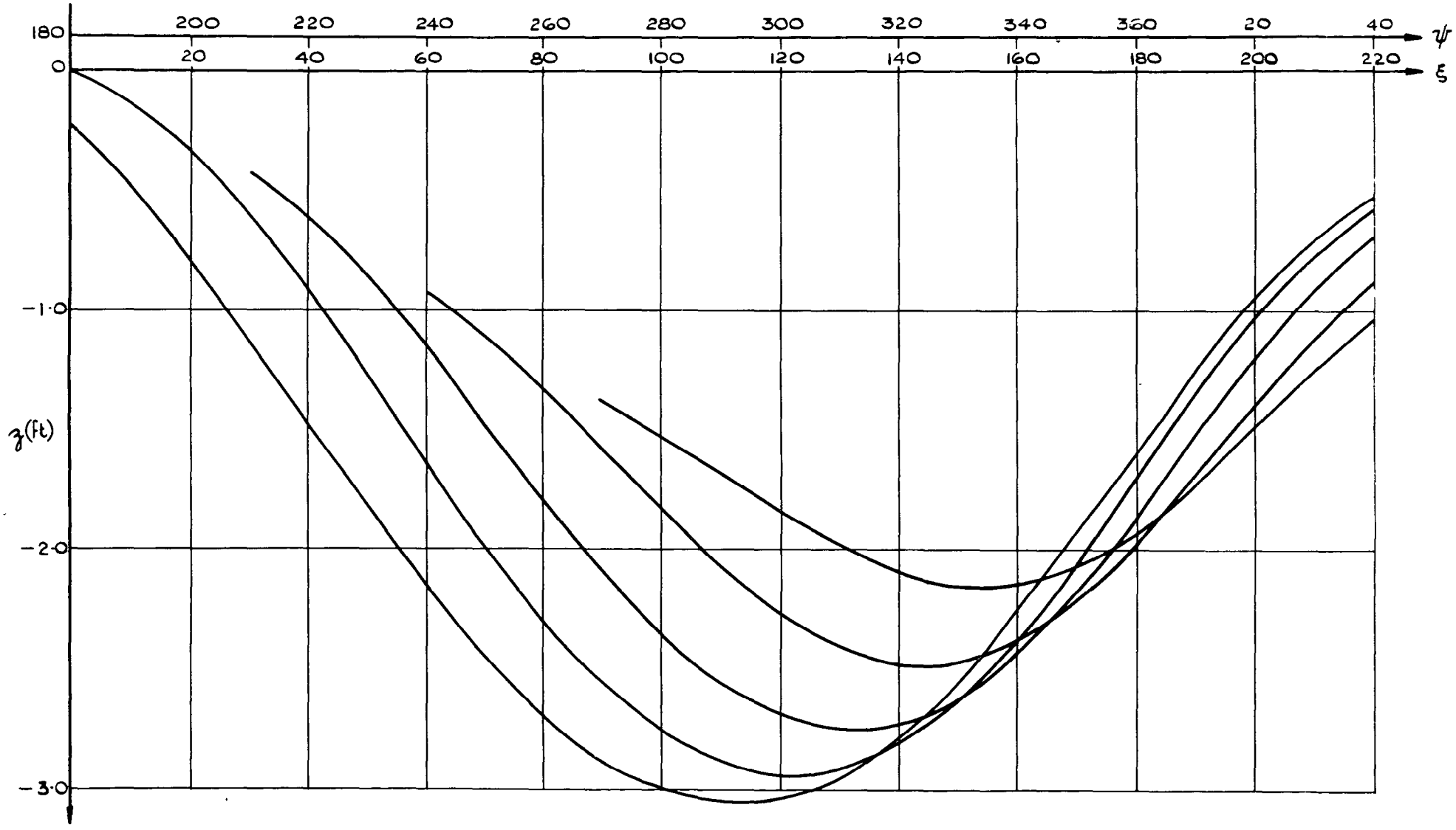

FIG. 22(a) TIP DEFLECTION OF WHIRLWIND ROTOR IN 30KT. WIND HIT BY A 5ft/sec. DOWNWARD GUST ($\Omega = 4$ rads./sec.)

Printed in England for Her Majesty's Stationery Office by the Royal Aircraft Establishment, Farnborough. Dd.125875. K.4.

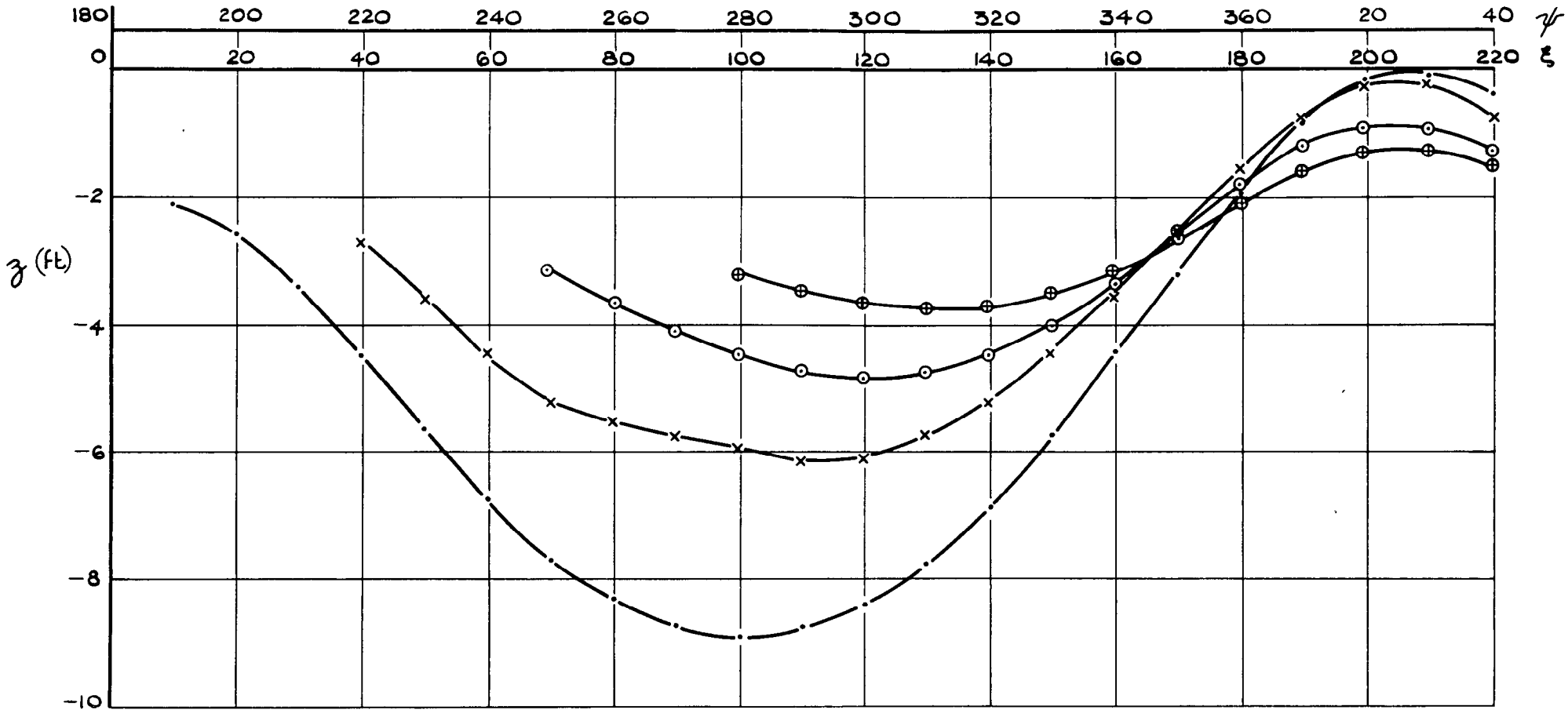

FIG. 22(b) TIP DEFLECTION OF WHIRLWIND ROTOR IN 30KT. WIND HIT BY 5 ft./sec. DOWNWARD GUST (Ω=2 rads./sec.)

A.R.C. C.P. 852

THE MOTION OF HELICOPTER BLADES AT LOW ROTOR SPEEDS IN HIGH WINDS

Willmer, M. A. P. September 1963.

A theory for predicting the behaviour of a rotor at low r.p.m. in a strong steady wind has been developed. Results have been obtained both for helicopters on the ground and on a rolling platform. It has been found that, under steady conditions and with the helicopter on the ground, serious blade deflections are not likely to occur. However, with a helicopter on a raised landing deck, it is possible for the 'cliff-edge' effect to be of major importance especially for helicopters with large rotors relative to the deck width. Finally the blade response to a vertical gust has been investigated and it has been shown that helicopter rotors are very susceptible to them.

A.R.C. C.P. 852

THE MOTION OF HELICOPTER BLADES AT LOW ROTOR SPEEDS IN HIGH WINDS

Willmer, M. A. P. September 1963.

A theory for predicting the behaviour of a rotor at low r.p.m. in a strong steady wind has been developed. Results have been obtained both for helicopters on the ground and on a rolling platform. It has been found that, under steady conditions and with the helicopter on the ground, serious blade deflections are not likely to occur. However, with a helicopter on a raised landing deck, it is possible for the 'cliff-edge' effect to be of major importance especially for helicopters with large rotors relative to the deck width. Finally the blade response to a vertical gust has been investigated and it has been shown that helicopter rotors are very susceptible to them.

A.R.C. C.P. 852

THE MOTION OF HELICOPTER BLADES AT LOW ROTOR SPEEDS IN HIGH WINDS

Willmer, M. A. P. September 1963.

A theory for predicting the behaviour of a rotor at low r.p.m. in a strong steady wind has been developed. Results have been obtained both for helicopters on the ground and on a rolling platform. It has been found that, under steady conditions and with the helicopter on the ground, serious blade deflections are not likely to occur. However, with a helicopter on a raised landing deck, it is possible for the 'cliff-edge' effect to be of major importance especially for helicopters with large rotors relative to the deck width. Finally the blade response to a vertical gust has been investigated and it has been shown that helicopter rotors are very susceptible to them.

DETACHABLE ABSTRACT CARDS

Published by
HER MAJESTY'S STATIONERY OFFICE
To be purchased from
49 High Holborn, London W.C.1
423 Oxford Street, London W.1
13A Castle Street, Edinburgh 2
109 St. Mary Street, Cardiff
Brazennose Street, Manchester 2
50 Fairfax Street, Bristol 1
35 Smallbrook, Ringway, Birmingham 5
80 Chichester Street, Belfast 1
or through any bookseller

C.P. No. 852

S.O. CODE No. 23-9016-52